65-280

1727-FR2

FINAL REPORT

GG159C MINIATURE INTEGRATING HIGH "g" GYRO
GG159C TORQUER STUDY
GG159C HIGH-FREQUENCY FLUID PUMP STUDY

California Institute of Technology
Jet Propulsion Laboratory
Pasadena, California

JPL Contract No. 950604 Modification No. 3

23 April 1965

HONEYWELL Aeronautical Division

Aero Report 1727-FR2

April 1965

FINAL REPORT

DEVELOPMENT PROGRAM FOR A HIGH FREQUENCY PUMP AND HYDROSTATIC SUSPENSION FOR THE GG159C GYRO

Jet Propulsion Laboratory
Contract No. 950604

Prepared by:

R. F. Anderson
Senior Development Engineer

Approved by:

R. G. Baldwin
Project Engineer

M. H. Riesgraf
Section Head
Low Cost Components

R. C. Amos
Project Administrator
Program Management

This work was performed for the Jet Propulsion Laboratory, California Institute of Technology, sponsored by the National Aeronautics and Space Administration under Contract NAS7-100.

Honeywell Inc.
Aeronautical Division
Minneapolis, Minnesota

CONTENTS

ILLUSTRATIONS

SECTION I
INTRODUCTION

The basic objective of the contract was the development of a high-frequency pump gimbal suspension system which meets turning rate and 'g' capability requirements of advanced space gyro applications. Main accomplishments of the contract were:

- Proper design of gimbal parameters for minimum reaction torque
- Selection of a compatible flotation fluid
- Reduction of pump power
- Increased pump excitation frequency to 400 cps

The GG159C gas spin bearing gyro utilizes a hydrostatically supported gimbal with the flotation fluid circulated by a fluid pump. Current production gyro pumps operate on 12.5-to 30-cps excitation frequency and require from 1.0 to 1.5 watts of power. The piezoelectric pump developed under this contract operates at 400 cps and has a power requirement of 0.2 watt. The gimbal suspension system was designed to meet JPL sterilization and high g requirements while simultaneously fulfilling the steady-state 15-g support and 15,000-deg/hr OA turning rate requirements with a satisfactory low gimbal damping (<2000 dyne/cm/sec).

A block diagram of the GG159 high frequency pump - suspension system is shown in Figure 1.

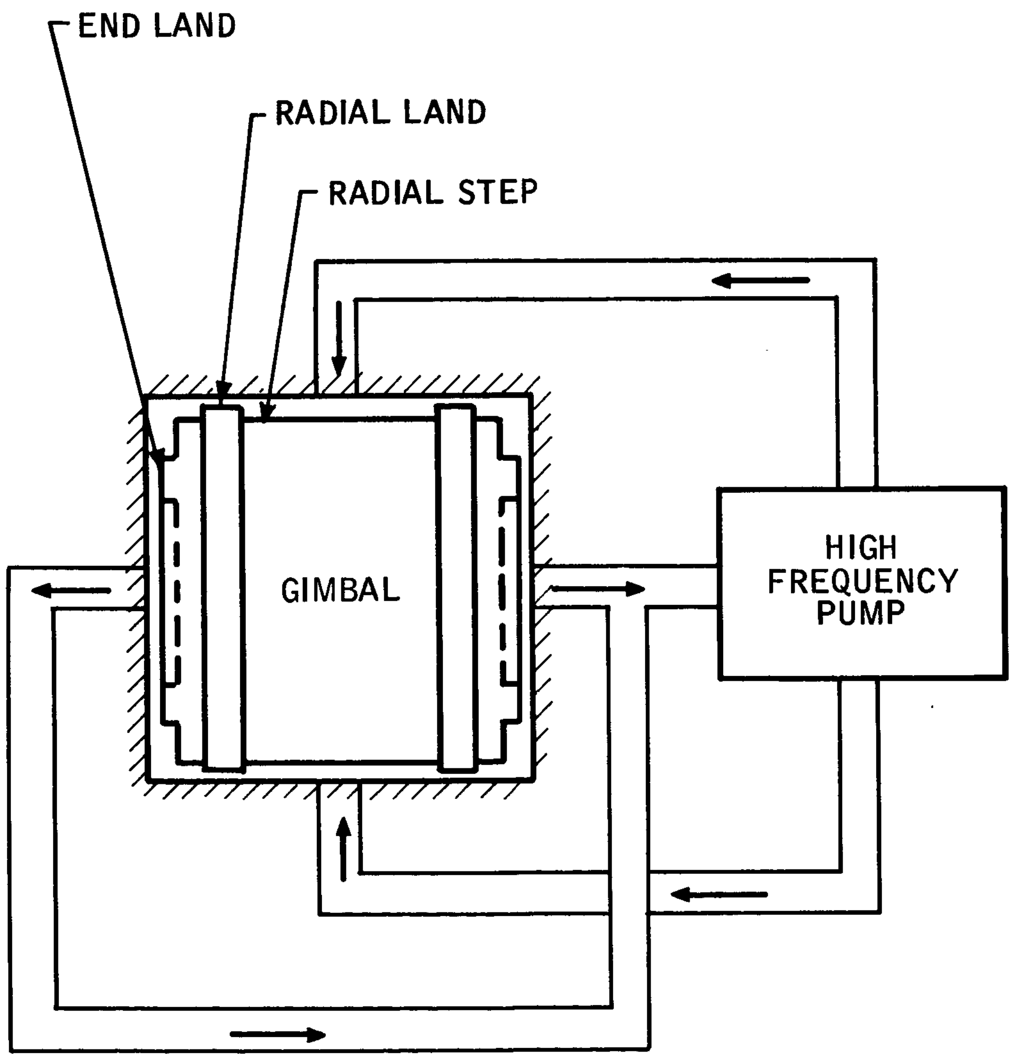

Figure 1. Gimbal Suspension System

SECTION II
CONTRACT SUMMARY

CONTRACT GOALS

The goal of this contract was to develop a high-frequency pump and suspension system for the GG159C gyro which would meet the following requirements:

- Support OA turning rate of 15,000 deg/hr
- Maintain gimbal stability for step-torque inputs
- Pump operation on 800 cps or 2400 cps power
- Piezoelectric dither or rotary-type pump consideration
- 15-G, steady-state support capability
- Minimum damping commensurate with support specifications.

These items were to be completed following the design study phase:

- Make layouts of suspension system and pump design
- Select the most feasible pump design
- Breadboard pump unit
- Test and evaluate pump for power, flow and pressure characteristics.

CONTRACT RESULTS

These goals were accomplished under the contract for the high frequency suspension and pump:

- Scaling of a suspension system which fulfills the 15,000 deg/hr turning rate specification, provides a 15-g gimbal support capability, maintains feasible gimbal clearances, and minimizes the damping (440 dyne-cm-sec at 130°F and 1770 dyne-cm-sec at 50°F).

- Scaling of a rotary pump concept which would provide the output required. This concept is feasible but has the inherent disadvantage of a high power requirement ($\sim$2.5 watts).

- Development of a piezoelectric pump consisting of a dither plate and a stationary plate, each having an orifice oriented in series to provide a rectified fluid flow large enough to support the proposed suspension system. The pump operates at 100 volts and 400 cps excitation frequency.

SECTION III
SUSPENSION SYSTEM

The hydrostatic suspension system for gimbal support requires consideration of the following parameters:

- OA turning rate (15,000 deg/hr)
- G capability (15 g's)
- Clearances
- Radial step gap to land gap ratio
- Step length to total length ratio
- End land radii ratio
- Pump delivery characteristic
- Fluid viscosity
- Gimbal length and diameter
- Fluid torques

The turning rate and g capability are per contract requirement. Fluid viscosity selection was governed by damping requirements and sterilization (300°F) specifications. Gimbal length and diameter are those of the GG159C gyro.

Design of a hydrostatically-supported fluid system requires an analysis of the radial support, axial and torsional supports, damping, and fluid torque. The fluid properties and geometric configuration must be selected and optimized to meet all requirements.

RADIAL SUPPORT

The radial support is given by the following equation:

$$\frac{F_R}{\epsilon} = \frac{36\mu Q\, r_g^{\,2}}{h_2^{\,3}} \left(\frac{1 - \alpha}{\alpha}\right) \left[\frac{\tanh \frac{KL}{2r_g} + \tanh \frac{(1-K)L}{2r_g}}{\alpha^3 \coth \frac{KL}{rg} + \coth \frac{(1-K)L}{r_g}}\right]$$

where

F_R = Radial load support, lb

ϵ = Eccentricity ratio (e/h_2)

h_2 = Radial land gap, inches

r_g = Radius to gap, inches

Q = Total fluid flow/2, in^3/sec

μ = Viscosity of fluid, $lb\text{-}sec/in^2$

α = Gap ratio (step gap/land gap)

K = Length ratio (step length/step plus land length)

L = Length of step plus land

Figure 2 shows curves for the radial support at 50°F and at 130°F for the suspension system. Note that the support is not quite optimized; however, parameter selection was also based on the damping curve shown in Figure 3.

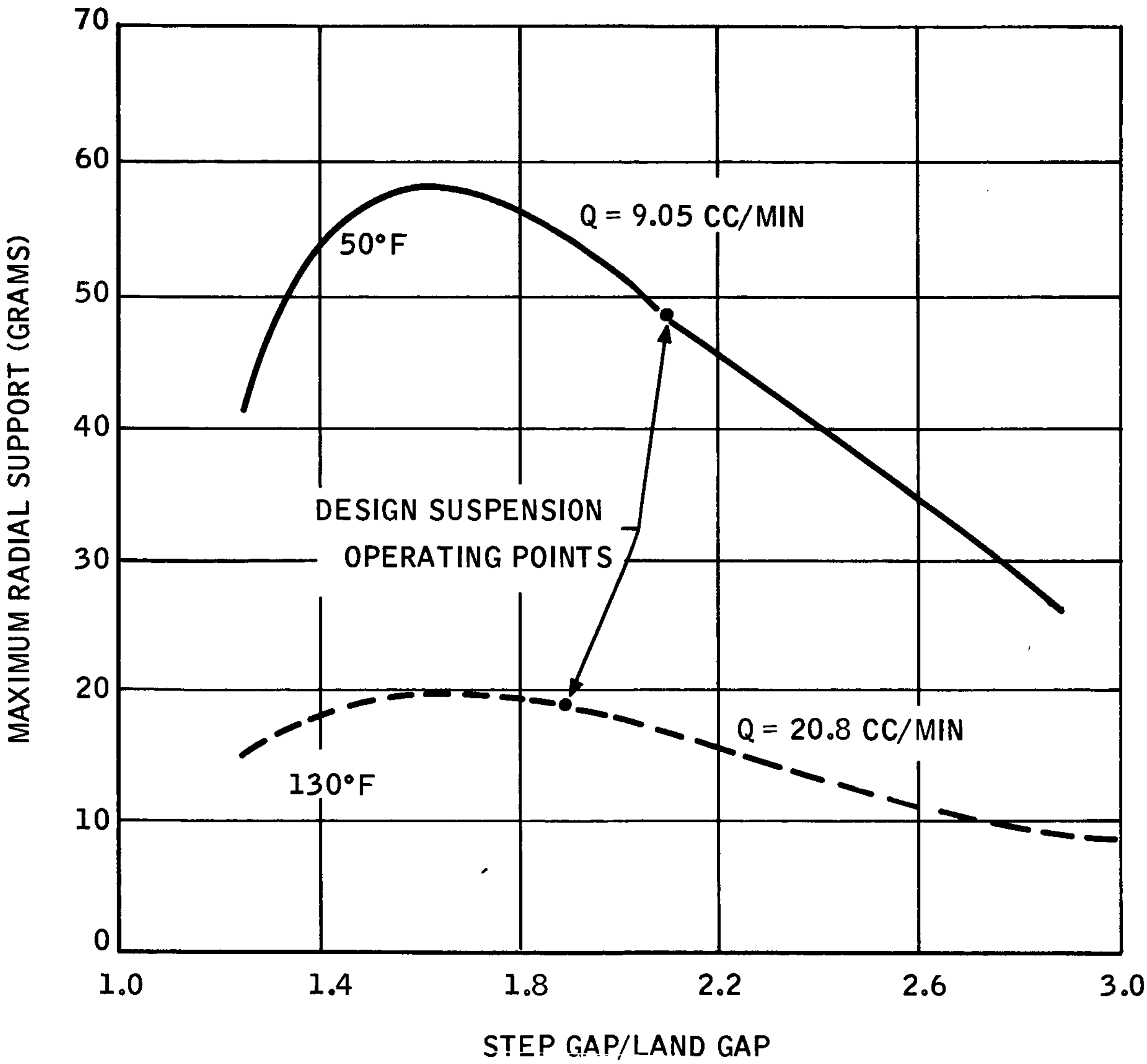

Figure 2. Suspension Radial Support

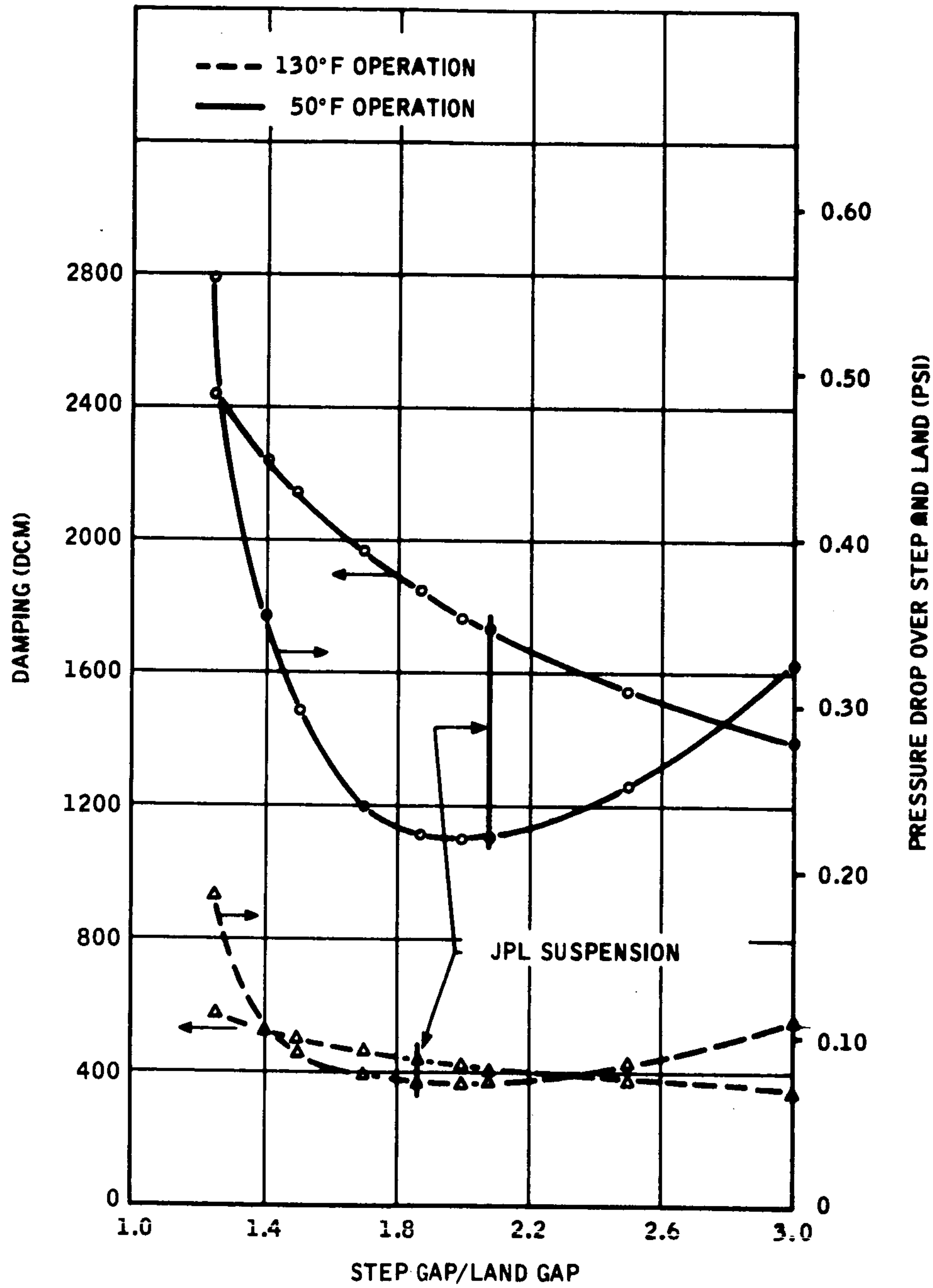

Figure 3. Damping - Pressure Drop Characteristic

Figure 4 shows the geometric support constant (K_G) as a function of clearance ratio for selected length ratios. The geometric constant is defined as

$$K_G = \left(\frac{1-\alpha}{\alpha}\right)\left[\frac{\tanh\frac{KL}{r_g} + \tanh\frac{(1-K)L}{r_g}}{\alpha^3 \coth\frac{KL}{r_g} + \coth\frac{(1-K)L}{r_g}}\right]$$

This result applies to general radial support scaling. If we maximize the geometric constant by computing the clearance ratio (α) for each length ratio (K) we get

K	α	K	α
0.50	1.44	0.75	1.56
0.55	1.46	0.80	1.60
0.60	1.48	0.85	1.68
0.65	1.51	0.90	1.78
0.70	1.53	0.95	2.08

Note that the suspension system values of 1.867 and 2.083 at 130°F and 50°F, respectively, do not optimize the support, but as mentioned earlier, are governed by the fluid torque ($\approx$ pressure drop) and damping considerations as shown in Figure 3.

Scaling results for radial support using the applicable parameters and including a factor for 15-g vector support of the gimbal can be reduced to

$$F_R = 5.15\ Q_T \text{ at } 50°\text{F}$$

$$\text{and } F_R = 0.856\ Q_T \text{ at } 130°\text{F}$$

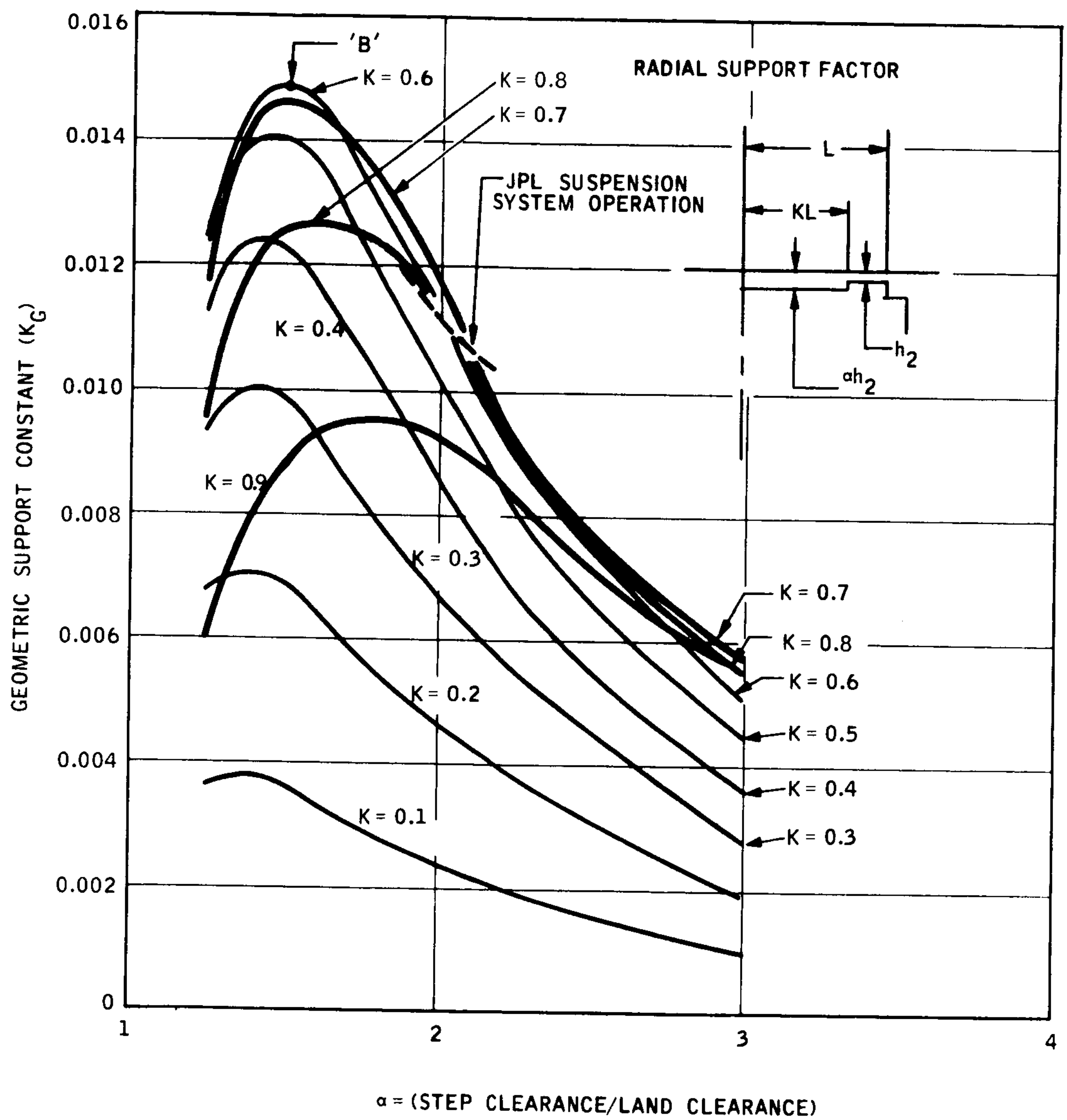

Figure 4. Gimbal Suspension System Radial Support (for constant flow condition)

AXIAL SUPPORT

The gimbal's axial support is obtained from two areas on the gimbal. The first portion of support force is derived from the pressure differential over the area outside the end land. This pressure differential is generated by the cylindrical restriction portion of the over-all fluid resistance as the flow is divided unequally when the gimbal moves off its center position. The second portion of the support is derived from the pressure drop across the end land.

When the flow divides unequally there is a reduction in radial support at one end of the gimbal. Computations showed that a 5.6 percent increase in flow is required to maintain 15 g's vectorially over that required for a direct radial loading of 15 g's. Figure 5 shows the support mechanism versus the 15-g specification.

The axial support is computed from the following equation which gives the force on the end of the gimbal.

$$F_A = \pi P_{o3} \left[r_o^2 - \frac{1}{2} \frac{r_1^2 - r_2^2}{\ell n \frac{r_1}{r_2}} \right]$$

Where P_{o3} is the pressure drop over the end land and can be computed from Equation (1).

A plot of the unequality of flow in each direction over the gimbal versus gimbal eccentricity is shown in Figure 6.

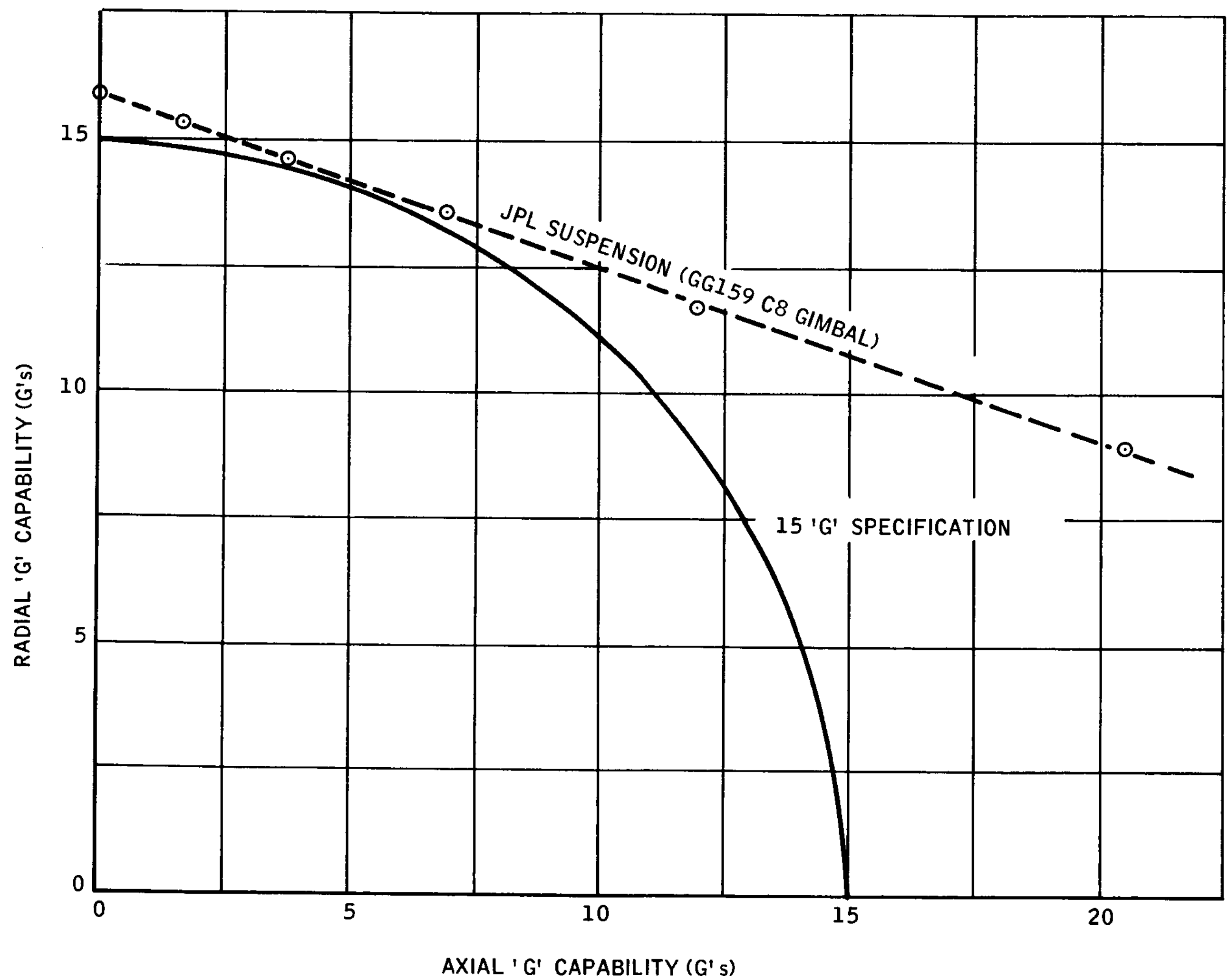

Figure 5. Gimbal "G" Loading Support

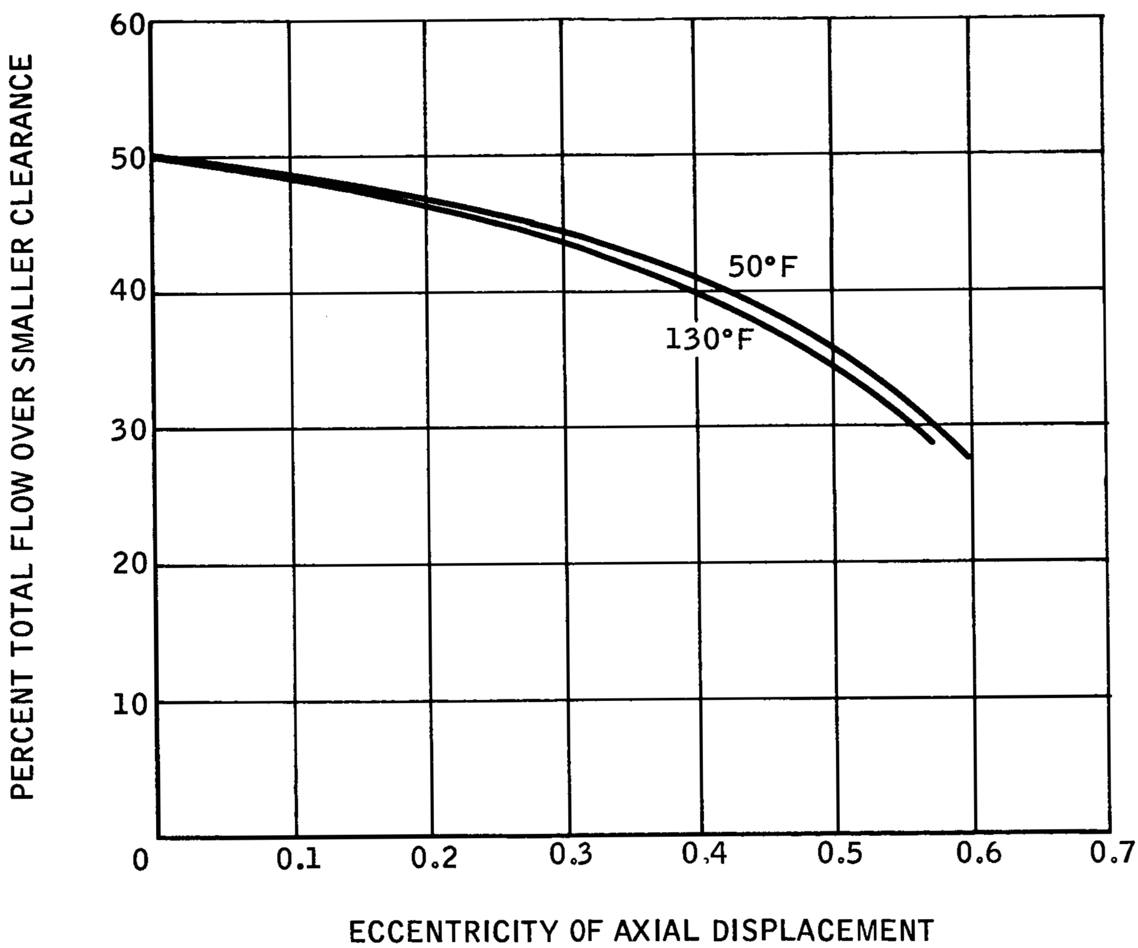

Figure 6. Fluid Flow Asymmetry

TORSIONAL SUPPORT

The torsional support required to meet the 15,000 deg/hr (4.17 deg/sec) OA turning rate specification is

$$T = \dot{\theta} H$$

$$= \frac{(15,000)(10^5)}{(3600)(57.3)(980)} = 7.42 \text{ gm-cm}$$

The torsional support computed for nominal JPL suspension parameters is

50°F	34.40 deg/sec
130°F	13.85 deg/sec

A plot of the torsional support for the suspension system over the operating temperature range is shown in Figure 7. Reference 1 covers a detailed derivation of the equations for gimbal torsional support.

DAMPING

The gimbal damping was computed using the equation:

$$D = 2\pi \mu \ r_g^3 \left[\frac{L_1}{h_1} + \frac{L_2}{h_2}\right] + \frac{\pi \mu}{h_3} (r_1^4 - r_2^4)$$

plus a small addition for large gap surfaces.

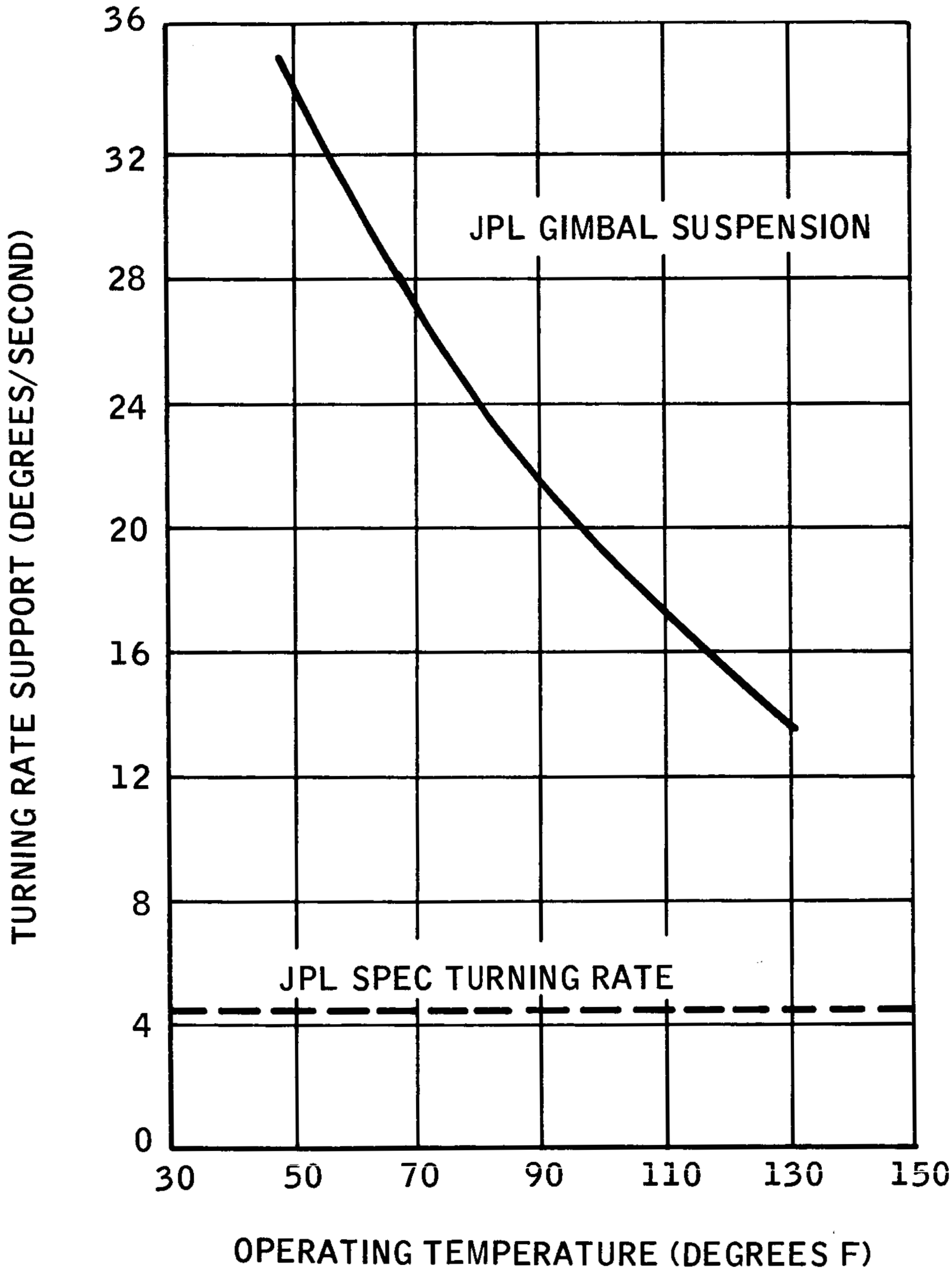

Figure 7. Torsional Support

The computed results are as follows:

Operating Temperature	Damping (dyne-cm-sec)
50°F	1770
70°F	1140
90°F	785
110°F	580
130°F	440

FLUID TORQUE AND PRESSURE DROP

Theoretical consideration shows that three sources of fluid torque exist in the GG159C hydrostatic suspension system. The parameters which combine to produce these torques are:

(1) a) Unfloatedness
    b) Deviation from axial straightness

(2) a) Axial weight unbalance
    b) Deviation from axial straightness
    c) Reciprocal of gimbal length

(3) a) Pressure drop over radial step and land
    b) Projected areas
    c) Deviation from axial straightness
    d) Tangential variation in film thickness

Most of these parameters are a function of fabrication techniques or are based on the gyro configuration. Gyro testing has indicated that the third torque noted above is the predominant magnitude for present GG159C units, and is almost directly proportional to the fluid flow or pressure drop over the gimbal. This torque can be minimized by limiting the pressure drop over the radial step and land to that required by the g specification. This is done by optimizing the geometric configuration.

The pressure drop over the radial step and land is:

$$P = \frac{12\mu Q}{\pi D}\left[\frac{L_1}{h_1^{\ 3}} + \frac{L_2}{h_2^{\ 3}}\right] \tag{1}$$

Substituting length and clearance ratios in the equation we get

$$\Delta P = \frac{6\mu Q_T L}{\pi D h_2^{\ 3}}\left[\frac{K}{\alpha^3} + (1-K)\right]$$

The pressure drop over the end land is

$$\Delta P = \frac{3\mu Q_T}{\pi h_3^3} \ln \frac{r_1}{r_0}$$

The pressure drops for the proposed suspension system are as follows:

	50°F	130°F
Radial Step	0.074	0.0345
Radial Land	0.154	0.0522
End Land	0.025	0.0108
Total Pressure Drop	0.0253 psi	0.0975 psi

The values are based on the minimum flows which will provide the 'g' support with nominal clearances. The step and lands are identified in Figure 8.

Evaluation testing at Honeywell has shown that the fluid torques are approximately proportional to the pressure drop (fluid flow). It is desirable that any suspension system have a minimum pressure drop across the radial land and radial step for the best gyro performance. Figure 9 shows the pressure drop as a function of the clearance ratio. Also shown are the flow requirements for 15-g radial support of the gimbal. Actual flow and pressure drop would be increased 5.6 percent to assure a 15-g vector support of the gimbal. Also indicated are the points of operation for the temperature extremes of 50°F and 130°F.

References 2 and 3 are a detailed analysis of the parameters contributing to fluid torque on a hydrostatically-supported gimbal.

LENGTH AND CLEARANCE RATIOS

As the step length to step plus land length ratio is nearly optimized in the present GG159C gyro, the present value of 0.812 was used. This is computed as the ratio of the 1.120 and 1.380 dimensions of Figure 8.

The radial step ratio is optimized by minimizing the pressure drop which will maintain the g capability. The pressure drop and damping as a function of the step to land clearance ratio are shown in Figure 3. Selection of the ratios considers both the desired minimums of fluid torques (proportional to pressure drop) and damping. The step gap clearances are 0.0050 at 50°F and 0.0056 at 130°F. The ratios (α) are 2.083 at 50°F and 1.867 at 130°F.

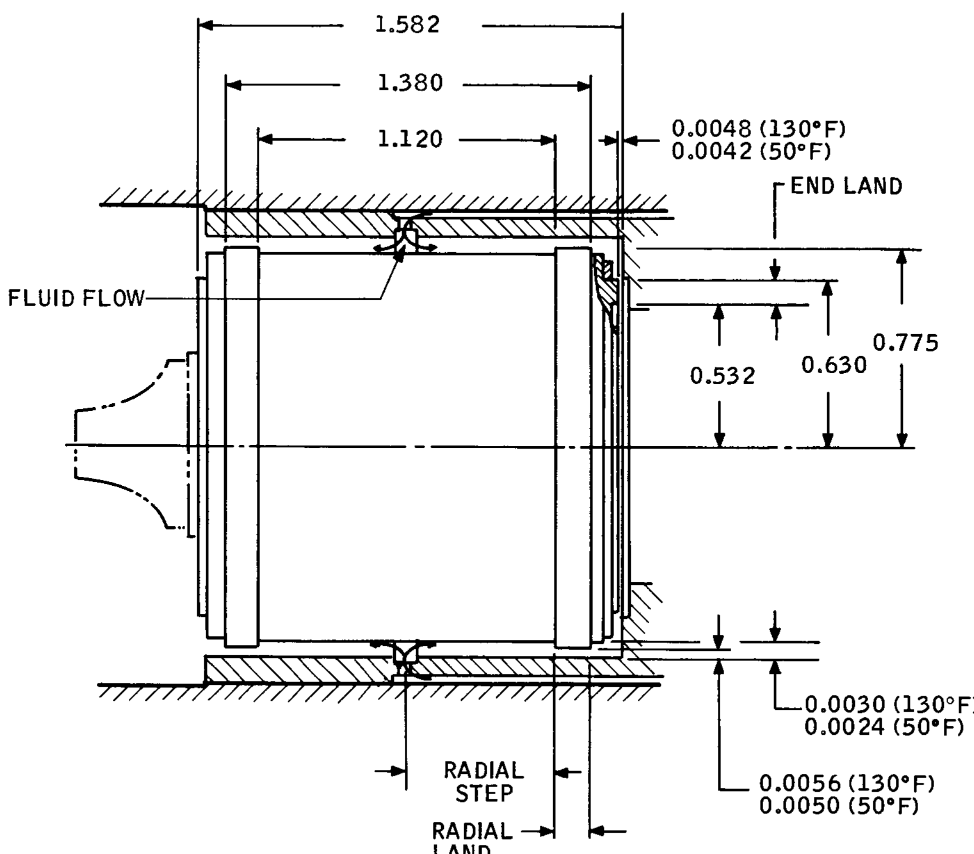

1 - FLOATATION FLUID: ALKANE 695
2 - VISCOSITY: 10 CENTIPOISES (50°F)
2.9 CENTIPOISES (130°F)
3 - FLOW REQUIRED: 9.05 CC/MIN (50°F)
20.5 CC/MIN (130°F)

Figure 8. JPL Gimbal Suspension System

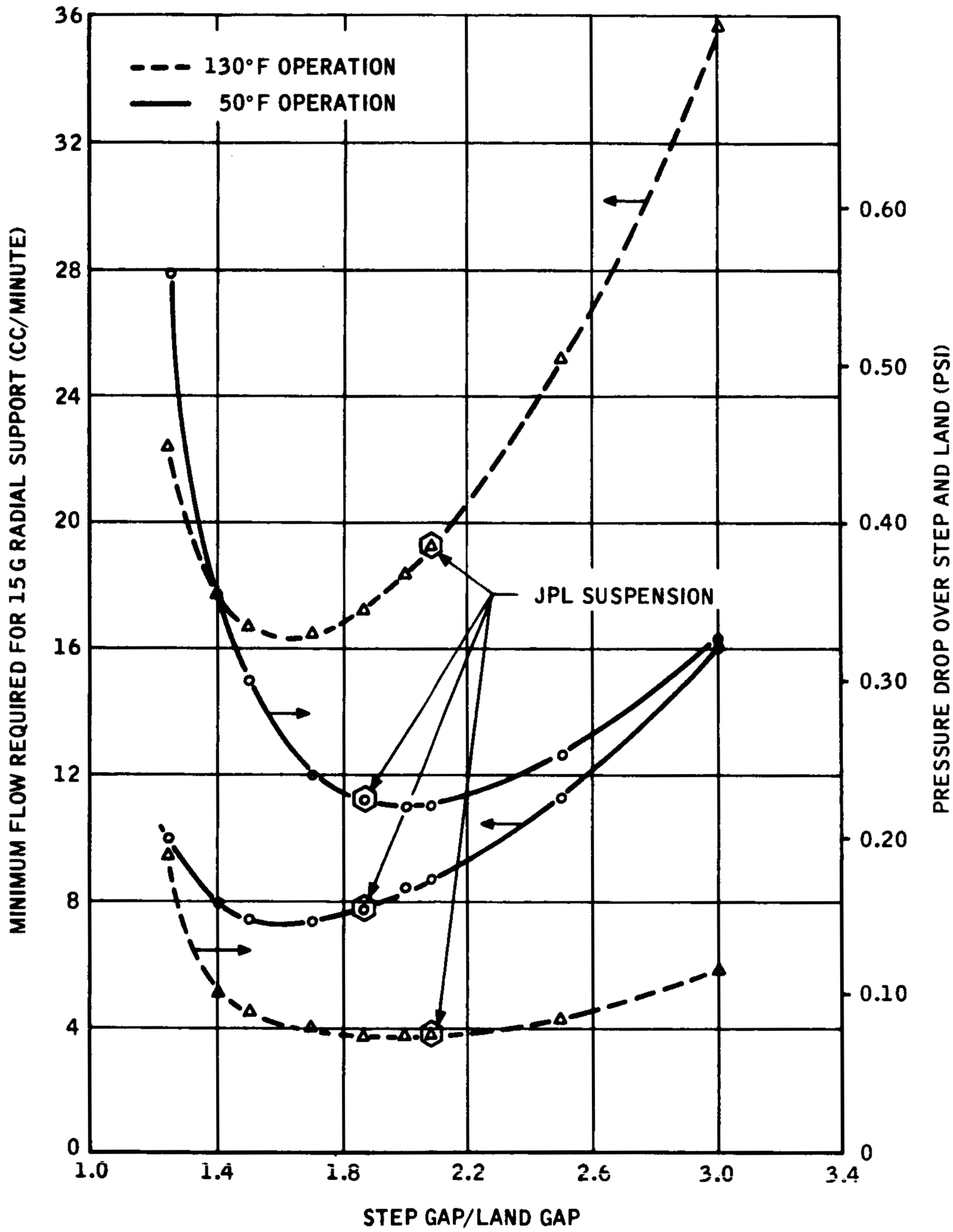

Figure 9. Fluid Flow - Pressure Characteristic

SUSPENSION FLUID

Initial gimbal scaling was based on use of Halocarbon No. 11-14 fluorolube which resulted in the following suspension properties:

	50°F	130°F
Viscosity (centipoises)	35.6	7.6
Gimbal damping (dyne-cm-sec)	6540	1200
Density	1.923	1.855
'G' capability (based on 0.2 gram unbalance)	24 g's radial 25 g's axial	
OA turning rate capability	18,400 deg/hr	

To achieve lower damping than the above values, the suspension system was rescaled with 1) low-viscosity suspension fluid and 2) 15-g capability specification over the 50°F to 130°F temperature range was added.

The properties of the Alkane 695 fluid are:

	50°F	130°F
Viscosity (centipoises)	10.0	2.9
Density	1.889	1.811
Thermal density coefficient	9.7×10^{-4} grams/cc/°F	
Boiling point	401°F	

These properties were used in the final scaling and pump flow-pressure requirements computed. The viscosity and gimbal damping over the operating range are shown in Figure 10.

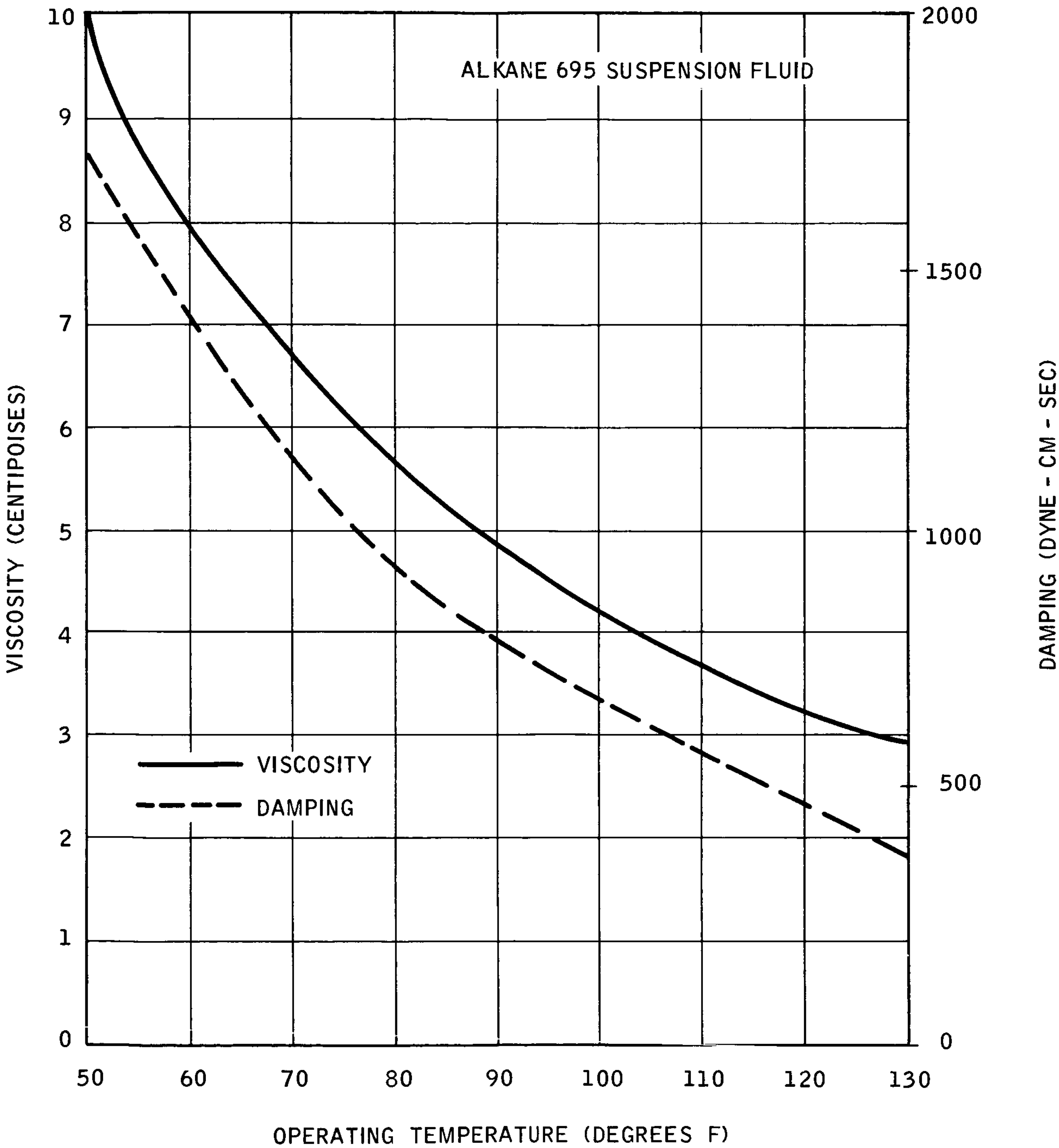

Figure 10. Damping and Viscosity versus Operating Temperature

CLEARANCES

The operating radial land clearance of the present GG159C is 0.0023. Based on this clearance and contamination considerations, a radial land clearance of 0.0024 at 50°F operation was selected for the JPL suspension system. Using expansion coefficients of 3.4×10^{-6} for ceramic (gimbal) and 13.1×10^{-6} for aluminum (gyro case) we compute the radial gap increase from 50°F to 130°F as

$$\frac{(13.1 - 3.4)(80)(1.553)}{(2)} = 0.0006$$

The radial land gap at 130°F is 0.0030.

GIMBAL UNFLOATEDNESS

The gyro gimbal assembly can be floated to a ±0.2-gram tolerance at any temperature datum. The datum selected is 110°F which results in a minimum 15g capability of the gimbal suspension over the 50°F to 130°F operating temperature range. The total unfloatedness is computed by taking the gimbal volume of 50 cc and taking the density change (9.7×10^{-4} grams/cc/°F).

$$(50)(9.7 \times 10^{-4})(80°\text{F}) = 3.88 \text{ grams}$$

Adding the total flotation tolerance of 0.4 gram, the total unfloatedness excursion for design consideration is 4.28 grams. Figure 11 shows the gimbal unfloatedness as a function of temperature. Using the 15g specification, the maximum gimbal support required is 46.65 grams at 50°F and 17.55 grams at 130°F.

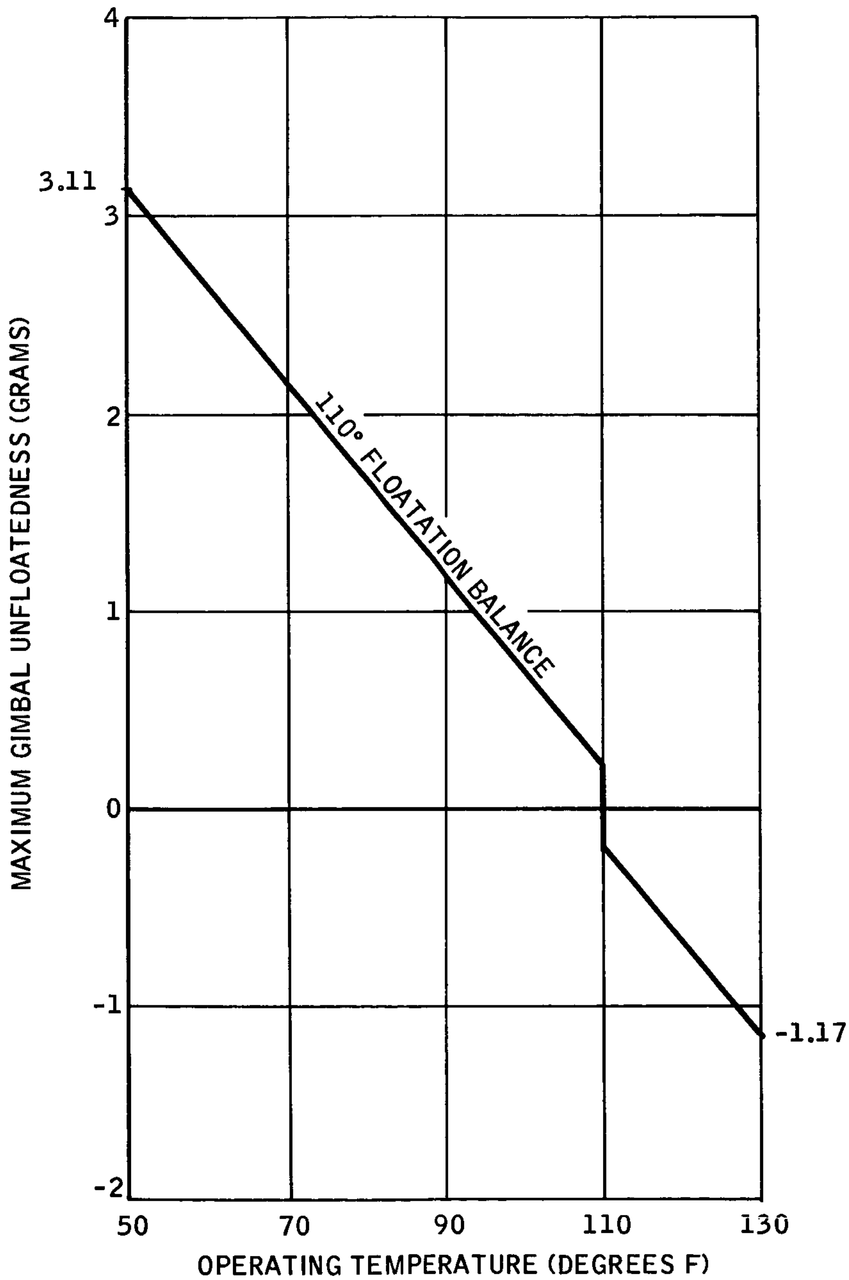

Figure 11. Gimbal Unfloatedness

SUMMARY OF SUSPENSION

Table 1 summarizes the properties and results of the scaling. Fluid flow and pressure are the minimum required to maintain the 15g specification.

Table 1. Suspension System

Suspension Factor	JPL Specification	50°F Datum	130°F Datum
OA Turning Rate (deg/sec)	4.17	34.4	13.85
'G' Capability (G's steady state)	15	15 minimum vectorially	
Damping (dyne-cm-sec)	Minimize	1770	440
Gimbal Clearances (In)			
Radial Step	--	0.0050	0.0056
Radial Land	--	0.0024	0.0030
End Land	--	0.0042	0.0048
Gimbal Unfloatedness (grams)	--	3.11	1.17
Length Ratio (K)	--	0.812	0.812
Clearance Ratio (α)	--	2.083	1.867
Fluid Flow (cc/min)	--	9.05	20.8
Viscosity (centipoises)	--	10.0	2.9

SECTION IV
ROTARY PUMP

The rotary pump considered for pumping the hydrostatic fluid has two possible configurations, as shown in Figure 12. The pump has inherently high power requirements because of the viscous drag of the drive element in the fluid. Power tradeoff of clearances versus power, use of high permeability materials, and the best pumping configurations still result in power requirements of approximately 2. 5 watts. Other than the high power requirements, the rotary pump design should provide enough outputs to support the suspension system.

DRIVE ELEMENT

It is desirable that the size of the motor be minimized so that it will fit inside the GG159C gyro configuration. This design requires some additional gyro length.

Scaling of a motor for a drive was predicated on scaling down torque curve of a No. 5 servo motor, increasing the stator o.d., and use of materials having higher saturation densities. Because of the low electrical-to-mechanical efficiency, the power levels are expected to be ~2. 5 watts in the operating range even after the above considerations.

Initial drive element scaling was accomplished by using a characteristic of the No. 5 motor and reducing the reference rotor length from 0. 57 to an applicable length of 0. 30. The motor curve used in the pump scaling was obtained by reducing the torque from a 400 cps No. 5 motor by the ratio of the rotor length reduction and doubling the speed intercept (800 cps versus 400 cps). This would result in a wattage requirement of ~3. 5 watts for a motor with a 0. 500 stator o. d.

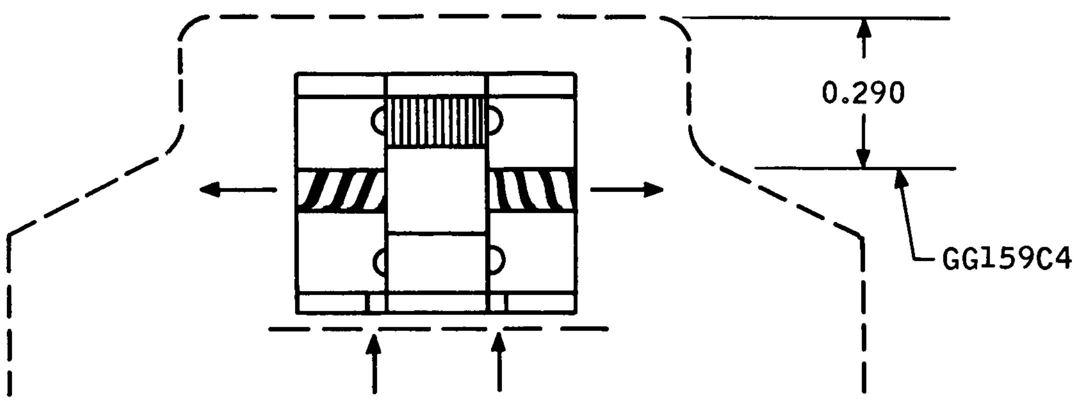

ROTARY PUMP - SEPARATE PUMP ELEMENTS

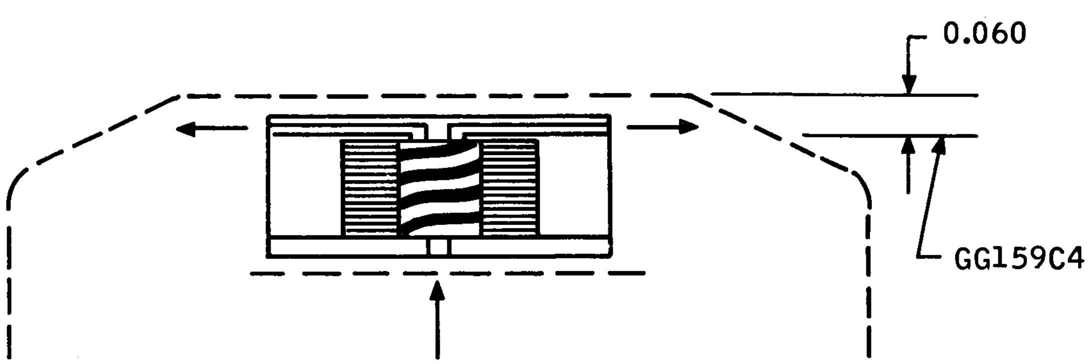

ROTARY PUMP - INTEGRAL PUMP-ROTOR

Figure 12. Rotary Pump Configurations

Substitution of Vanadium Permendur (50-50 cobalt iron) for the present Hipernik (50-50 nickel iron) as the stator and rotor material will allow saturation densities of 20,000 gauss, instead of 15,000 gauss. More torque can then be developed in the same iron volume, providing the basis for scaling down the length of the 400-cps, No. 5 induction motor to a 800-cps motor drive.

Increasing the stator element to 0.60-inch diameter would allow use of larger wire with an approximate 50 percent reduction in I^2R motor loss. An 0.60-inch diameter unit is the practical maximum size which could be designed into the present GG159C size configuration. With the reduction of 50 percent in I^2R losses, the net electrical power would then be from 2.2 watts at maximum efficiency (approximately the 130°F operating point) to 2.8 watts at stall for the design with separate pumping elements at each end of the drive element.

Using results of the following section on the Pumping Element for the design with integral pumping grooves on the motor rotor, an estimate is made for the power required to drive the rotor. The flux linkage from stator to rotor will be

$$\phi = \frac{N I \mu_p A}{h_r}$$

Assuming ϕ, N, μ_p, and A equal in both designs, the effective I/hr factors must be equal and can be approximated as

$$\frac{I_1 Lr}{h_r} = I_2 \left[\frac{Lr/2}{h_r} + \frac{Lr/2}{h_g}\right]$$

when h_r = nominal rotor clearance

h_g = nominal groove clearance

L_r = length of rotor

Using $h_r = 0.001$ and $h_g = 0.003$ we get

$$I_2 = 1.5 I_1$$

The power will be $\simeq I_2^2$ or

$$P_2 = (1.5)^2 P_1$$

From the above and scaling of a similar motor configuration $P_1 = 2.5$ watts and $P_2 \cong 6.25$ watts

Previous reporting showed a more favorable power comparison but groove depths used in the computation were too shallow to meet flow requirements.

A second rotary pump configuration will have the pumping grooves cut into the motor rotor as shown in Figure 10. The configuration was scaled using the above scaled-down No. 5 motor torque characteristic. Figure 13 shows the output characteristics together with the suspension requirements. As noted above, the power requirements are prohibitive for application of this design.

Table 2 is a summary of the rotary scaling for the two design configurations.

PUMPING ELEMENT

The rotary pumping elements have been scaled using the following theoretical formula developed in Reference 4 and experimental tests on a type thrust pump at Honeywell, Inc.

$$Q\ (\text{cc/min}) = (984)\ 2\pi\omega \frac{R}{h}^2 \frac{h^3}{\gamma + (1-\gamma) A^3}$$

$$A^3 - \gamma(1-\gamma)\sin^2\beta\,(A^3+1)^2 \qquad \frac{P_o h^2}{6\mu\omega RL} \qquad (2)$$

$$-\sin\beta\cos\beta\,\gamma\,(1-\gamma)(A^3-1)(A-1)$$

Table 2. Rotary Pump Design

Parameter	Separate Pump Elements	Rotor with Integral Grooves
DRIVE ELEMENT		
Radial Clearance	0.0010	0.0010
Axial Clearance	0.0020	0.001
Groove Helix Angle	--	45°
Groove Clearance	--	0.0030
Groove Length/Total Length	--	0.5
Length	0.30	0.30
Diameter	0.25	0.25
PUMPING ELEMENT		
Radial Clearance	0.0015	--
Groove Clearance	0.0105	--
Length (each end)	0.25	--
Groove Length/Total Length	0.5	--
Groove Helix Angle	15°	--
CURRENT RATIO	I_1	$1.5\ I_1$
POWER (WATTS)	2.5	6.25

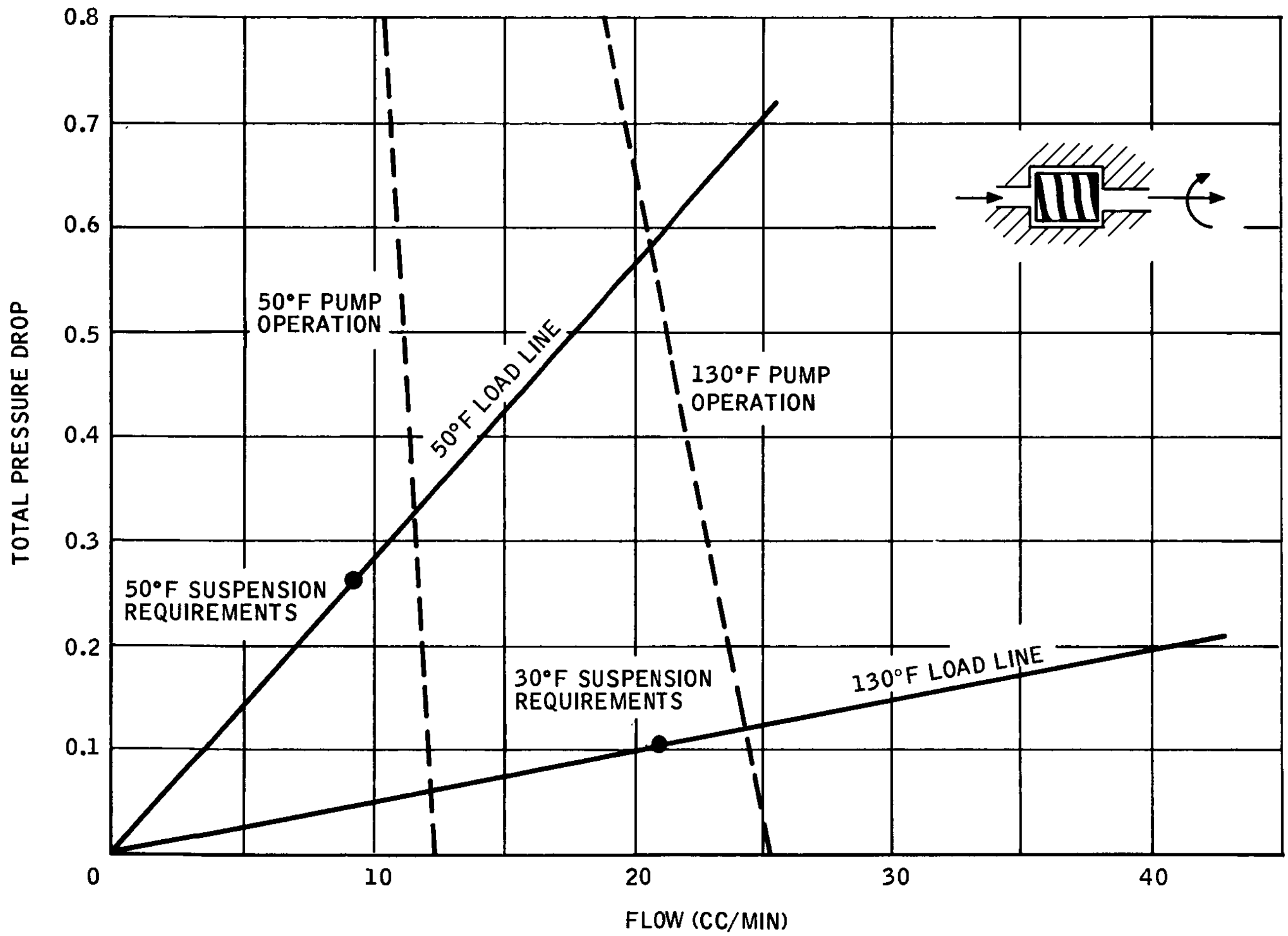

Figure 13. Rotary Pump Output - Integral Construction

The experiments have shown that the flow outputs at low pressures agree closely with theoretical calculations but the pressures at low flows (>> Q = 0) are about 50 percent of the calculated values. Therefore, a pressure intercept of 50 percent of the computed value is used at P = 0 to generate the pump characteristic.

For a rotary pump configuration having separate pumping elements at each end of the drive element the pressure-flow characteristics were computed at each 20°F temperature increment using the speed-drag characteristics from analysis of the rotating assembly and the motor load curve. Figure 14 shows a plot of these results.

Intersections of the suspension load lines with the pump characteristic determine the operating point at each temperature. These flows, in turn, are used to calculate the load support and torsional stiffness.

The drag of the pumping element or driving element is computed from the cylindrical drag equation

$$D = \pi \mu R^3 \omega \left[\frac{2L}{h_j} + \frac{R}{h_e}\right]$$

For the drive element of the configuration using separate pumping elements we have

$$D = \pi \mu (0.125)^3 \omega \left[\frac{2(.30)}{0.001} + \frac{0.125}{0.002}\right] (1.13 \times 10^6)$$

$$= 4.59 \times 10^6 \mu \omega \text{ (in dyne-cm)}$$

For the pumping elements the drag is

$$D = \pi \mu (0.06)^3 \omega \left[(2)(2)\left(\frac{0.125}{0.0015} + \frac{0.125}{0.0105}\right) + \frac{0.060}{0.002}\right] (1.13 \times 10^6)$$

$$= 0.32 \times 10^6 \mu \omega \text{ (in dyne-cm)}$$

The total drag for the combined rotary element is

$$D_T = 4.91 \times 10^6 \mu\omega$$

Figure 14 shows the drag characteristic plots for five temperatures.

From the motor characteristic curve with an equation of approximately

$$D = 4085 \left(1 - \frac{N}{19000}\right)$$

in the above drag relationship the intercepts (operating points) can be computed for the pump at several operating temperatures.

Temperature	Fluid Viscosity (Lb-Sec/In^2)	Drag Dyne-Cm	Speed (RPM)	Mechanical Power (Watts)
50°F	1.45×10^{-6}	3165	4250	0.135
70°F	0.97×10^{-6}	2860	5730	0.164
90°F	0.696×10^{-6}	2550	7130	0.182
110°F	0.53×10^{-6}	2280	8380	0.191
130°F	0.42×10^{-6}	2045	9470	0.194

From the values of viscosity and speed, the flow and pressure can be computed from Equation (2). The results are as follows, noting the pressures as 50 percent of those computed.

	Q (at P=0) (cc/min)	P (at Q=0) (Psi)
50°F	12.9	0.84
70°F	17.4	0.75
90°F	21.6	0.67
110°F	25.4	0.60
130°F	28.7	0.54

Figure 15 shows the 50°F and 130°F pump characteristics superimposed on the suspension requirement load lines.

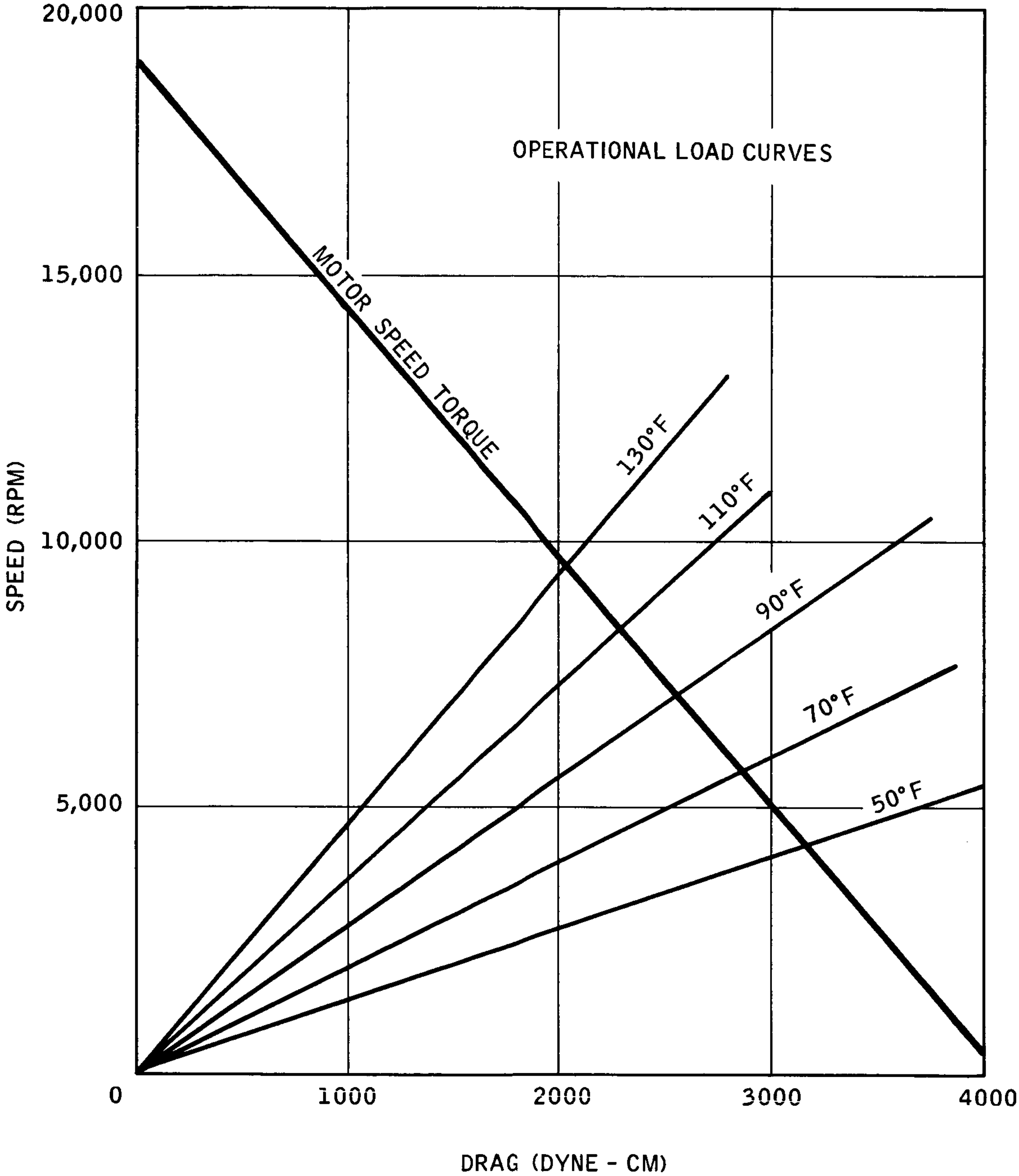

Figure 14. Rotary Pump Speed - Torque Characteristics

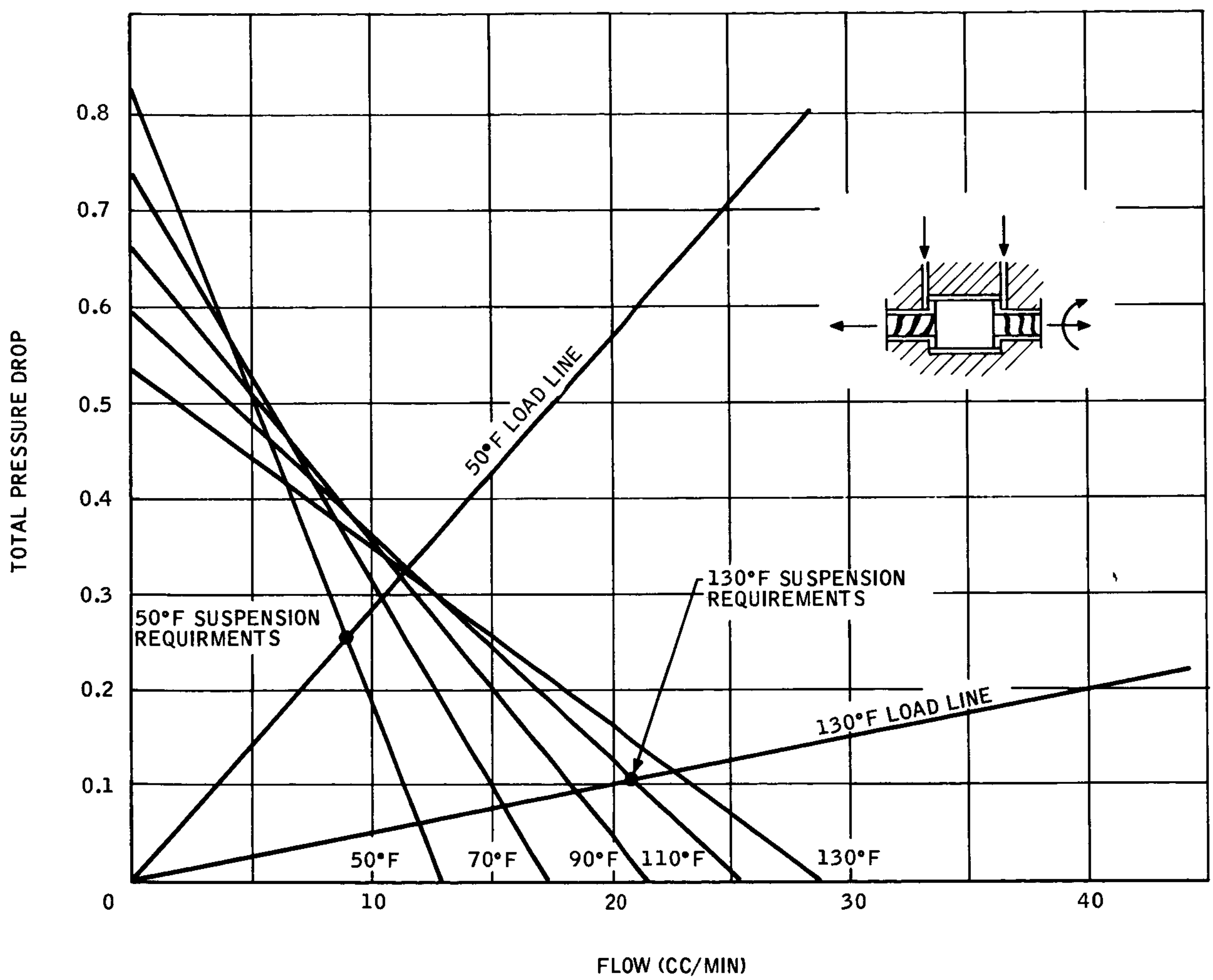

Figure 15. Rotary Pump Output - Separate Pumping Element

Advantages of the separate pumping element concept are:

- Less power (2.5 versus 6.4 watts) due to maintenance of uniform clearance in radial air gap of rotor.
- Less critical tolerances. Small variations in radial gap and groove clearance result in larger changes in pump characteristics.
- Axial support of rotor is easily achieved with flow over the ends of rotor in both directions, resulting in opposite pressure loads. With single direction flow a more refined design is required for axial support.

Disadvantages of the separate pumping element concept are:

- Additional length of gyro would be 0.290 versus approximately 0.060 for patterned rotor pump.
- More piece part alignments required for fabrication.

In general, the separate pumping element concept can be expected to give more consistent pumping results from unit to unit for like tolerances. For example, this can be noted by considering the effects of a ±0.0001 tolerance on the respective 0.0105 versus 0.0030 groove clearances.

Figure 16 shows a layout of the separate pumping element configuration as integrated into the GG159C gyro.

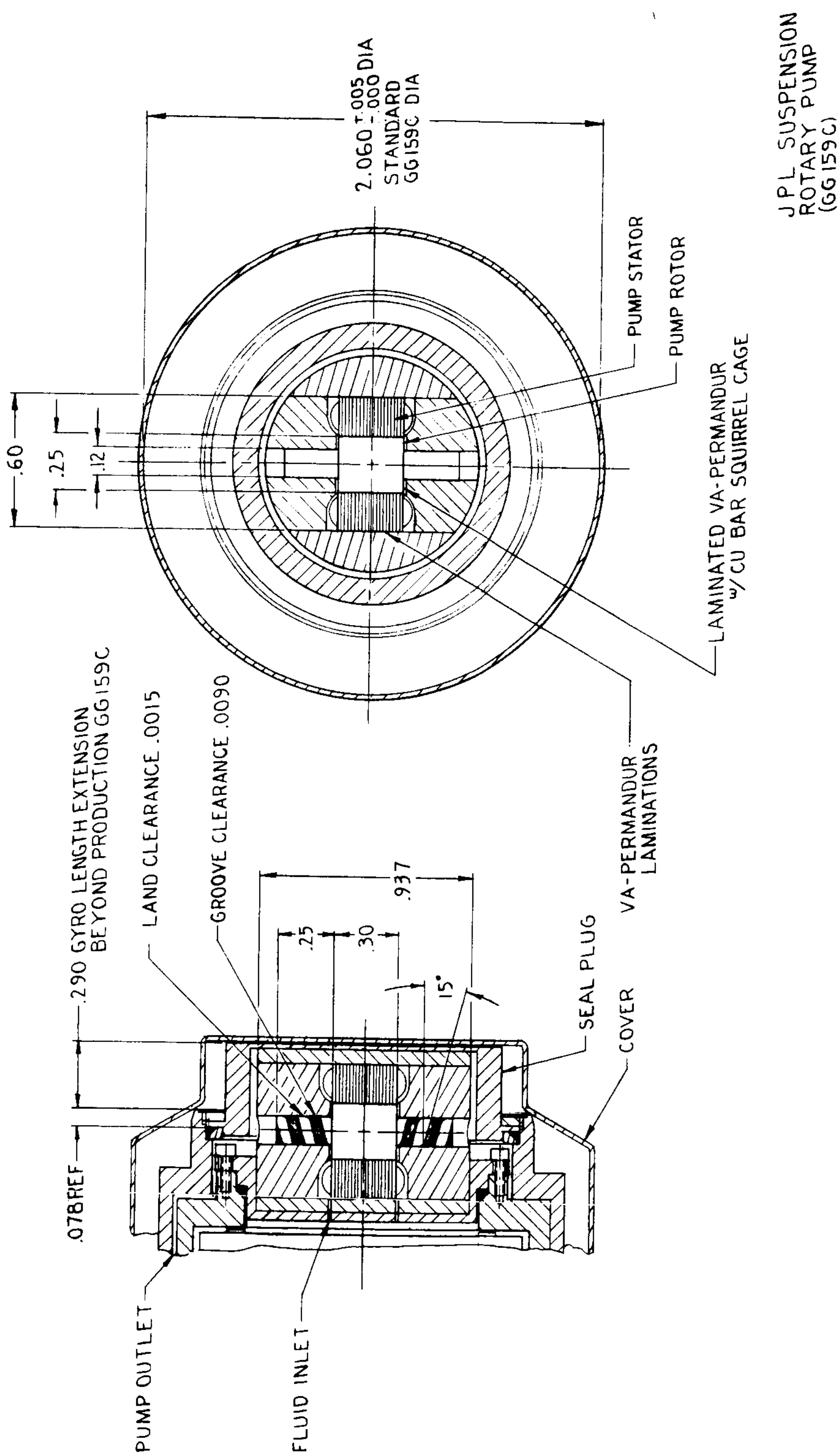

Figure 16. Rotary Pump Layout

SECTION V
PIEZOELECTRIC PUMP

Use of a piezoelectric dither assembly as a high frequency pump was studied. The disc assembly consists of a thin (~ 0.003-inch) brass shim bonded between two conductive lead-coated zirconate titanate ceramic plates. The ceramic plates are oriented in polarity and a conductive epoxy is used in some areas of the bonding to assure uniform conductivity to the surfaces of the plates. Leads are attached to the brass shim and to terminals connected in series to the outside surfaces of the assembly. Figure 17 shows the cross section of the piezo disc assembly.

The piezoelectric plates contract and expand cyclically in a radial direction when an a-c potential is applied in an axial direction. The polarities of the plates are oriented oppositely from center to outside so that the a-c potential will cause a bi-metal flexing of the plates with reversals at the frequency of excitation. This motion is used in developing the high-frequency fluid flow.

GENERAL ASSEMBLY

The piezo pumping plate assembly consists of two ceramic discs, a brass spacer, and terminals. High temperature conductive epoxy (Spec 7556A) is used at a few spots on each side of the brass shim and to fix the terminals to the conductive coating on the ceramic plates. The coating on the plates is fired on to a thickness of 0.0005 to 0.0015 on each side of each plate. A high-temperature epoxy (Spec 6293F) is used to bond all remaining surfaces and insulate terminals. The assembly is ~0.053 thick after complete fabrication.

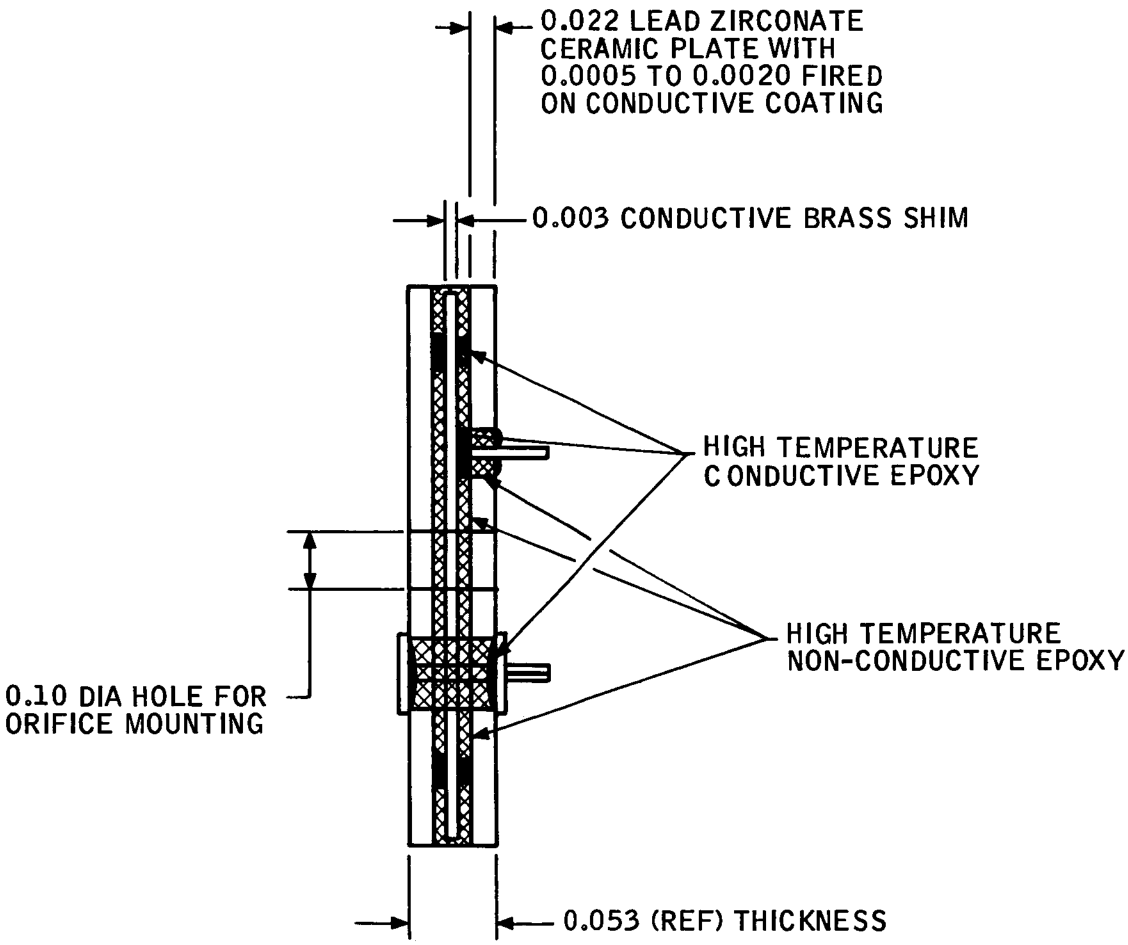

Figure 17. Piezo Pumping Plate Assembly

FLOW RECTIFICATION

Several methods of rectifying the fluid displaced by the dither disc assembly were considered. Most types of check valves, flow rectifiers, and plate-to-rectifier arrangements have limited practicability because of space in the gyro or poor frequency response at 800 cps.

The method used for scaling and development is that of mounting an orifice in the center of the piezoelectric disc assembly and using a second aligned orifice mounted in a stationary plate. The second orifice is oriented in the same direction as the piezo pumping orifice and o-rings are used as sealing and mounting between the plates.

VISCOSITY EFFECTS ON PUMPING

The pump was checked using fluids having viscosities of 1.4 and 17.0 centipoises in addition to the Heptacosa (5 centipoises). No large change in pump performance with viscosity was noted although some degradation will occur at high flows for the 1.4 centipoise fluid. The pump output is ample to meet requirements of the suspension system. The fluids used were flourolube blends whose viscosity values encompass the proposed operating range of viscosity of the Alkane 695 suspension fluid (10 cp at 50°F to 2.9 cp at 130°F). Figures 18 and 19 show the static head (no flow) versus frequency and the 400-cps pump characteristics for the three fluids derived from laboratory tests.

PLATE MOTION AND PHASE LAG VERSUS RADIAL POSITION

As part of the study of pumping parameters, the peak-to-peak motion of the piezo plate assembly at radial points of the plate and the phase lag of the peak amplitude with respect to the excitation voltage input were measured

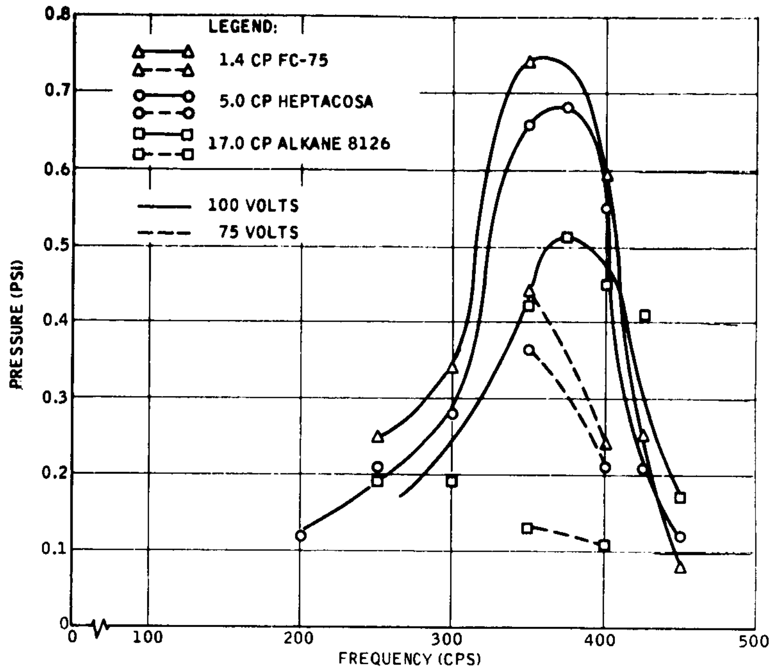

Figure 18. Static Head versus Frequency

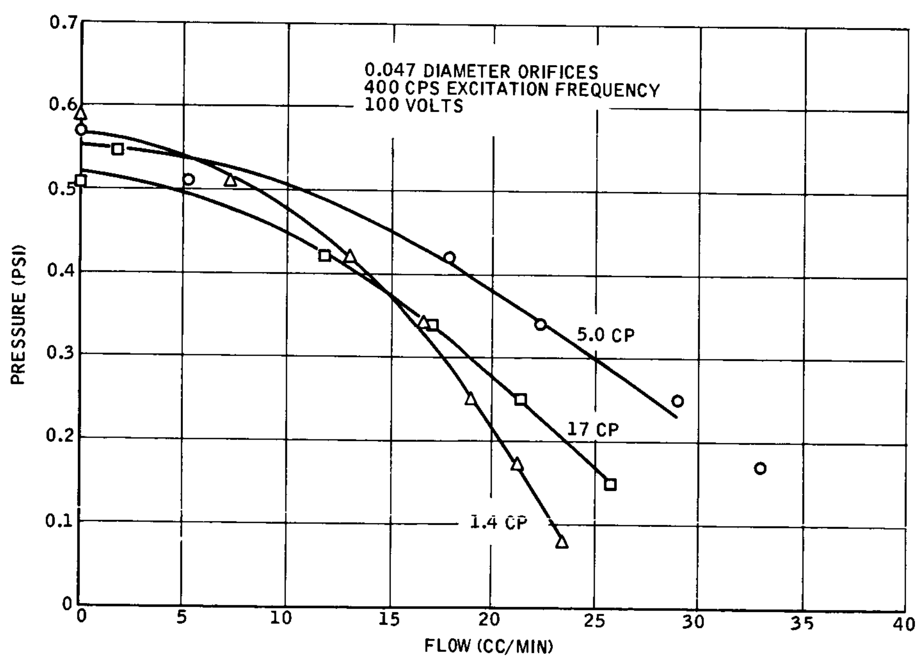

Figure 19. Flow versus Viscosity

and are depicted on the plots of Figures 20 and 21. The predominant motion is spherical "dishing" of the plate as might be expected. However, there was a small waviness in the profile of the plate motion in addition to the "dishing", as can be noted from the change in phase relation of the radial position peaks with respect to each other. At the high frequencies the plate moves in phase with the input excitation frequency.

PLATE DEFLECTIONS

The piezoelectric plate assembly must have a certain threshold of peak-to-peak motion before pumping is initiated. After this threshold is reached the pumping increases somewhat linearly with voltage up to 100 volts or above.

Plate deflections were monitored with a capacitance probe. The probe was set up in a micrometer transducer and calibrated at a position approximately 0.005 from the plate. The probe was set at a distance of ~10 times the peak-to-peak plate amplitude to readout non-linearity while maintaining feasible sensitivity. The peak-to-peak motion was measured from the transducer output through a dynagage.

Figure 22 shows the plate deflections for the 400-cps and 800-cps pump assemblies as mounted in the test mockup. Note that the maximum deflections are at a frequency slightly below that of the reference output frequency. Checks indicated that the threshold peak-to-peak motion for pumping is less at 350 cps than at 400 cps.

PIEZOELECTRIC PLATE MOUNTING

The best pumping results were obtained when the piezo plate assembly and rectifier plates were mounted with 0.070 cross-sectional diameter x 1.25 o.d. major diameter o-rings between the plates and on each side of the complete

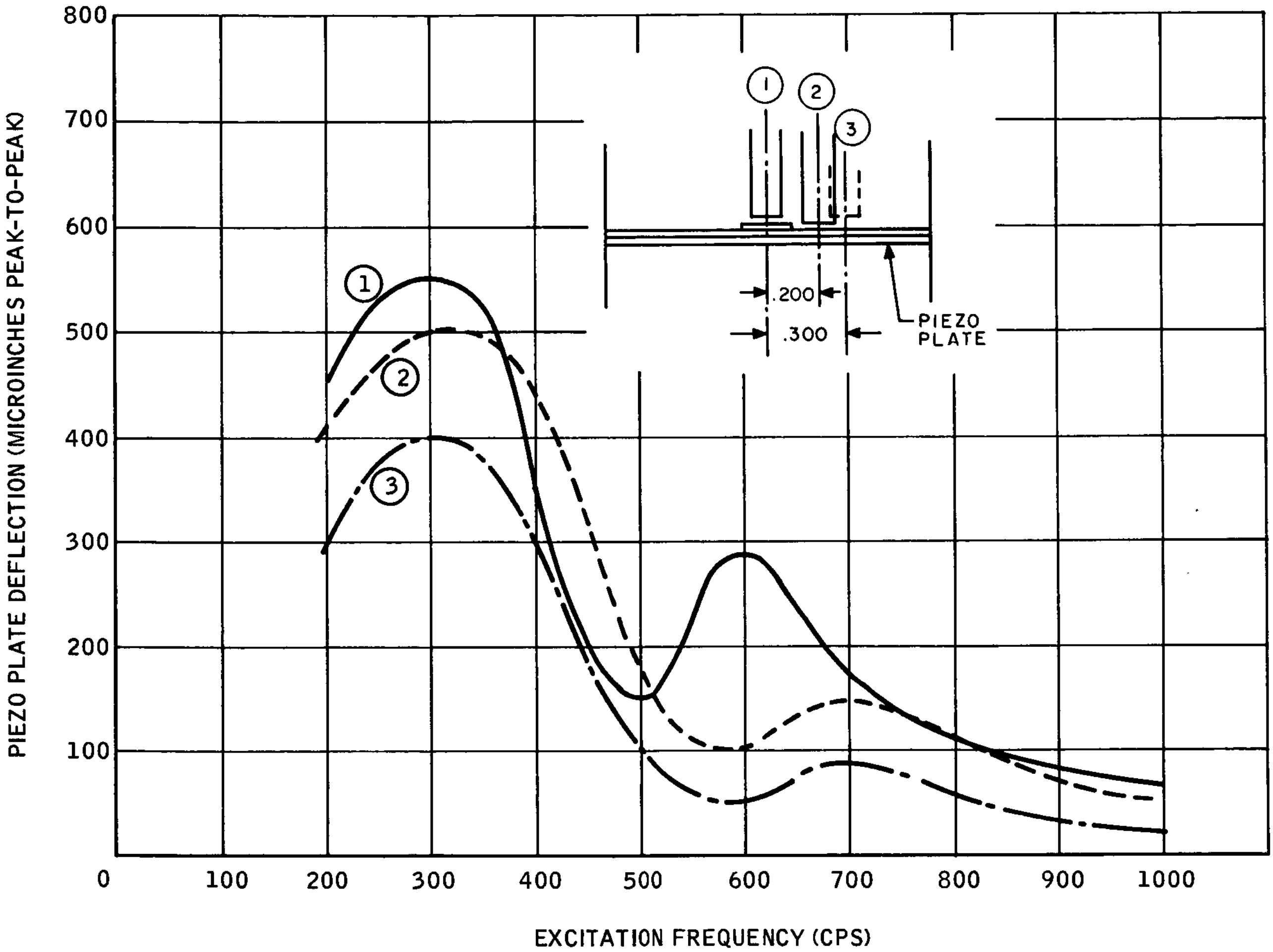

Figure 20. Deflection versus Radial Position

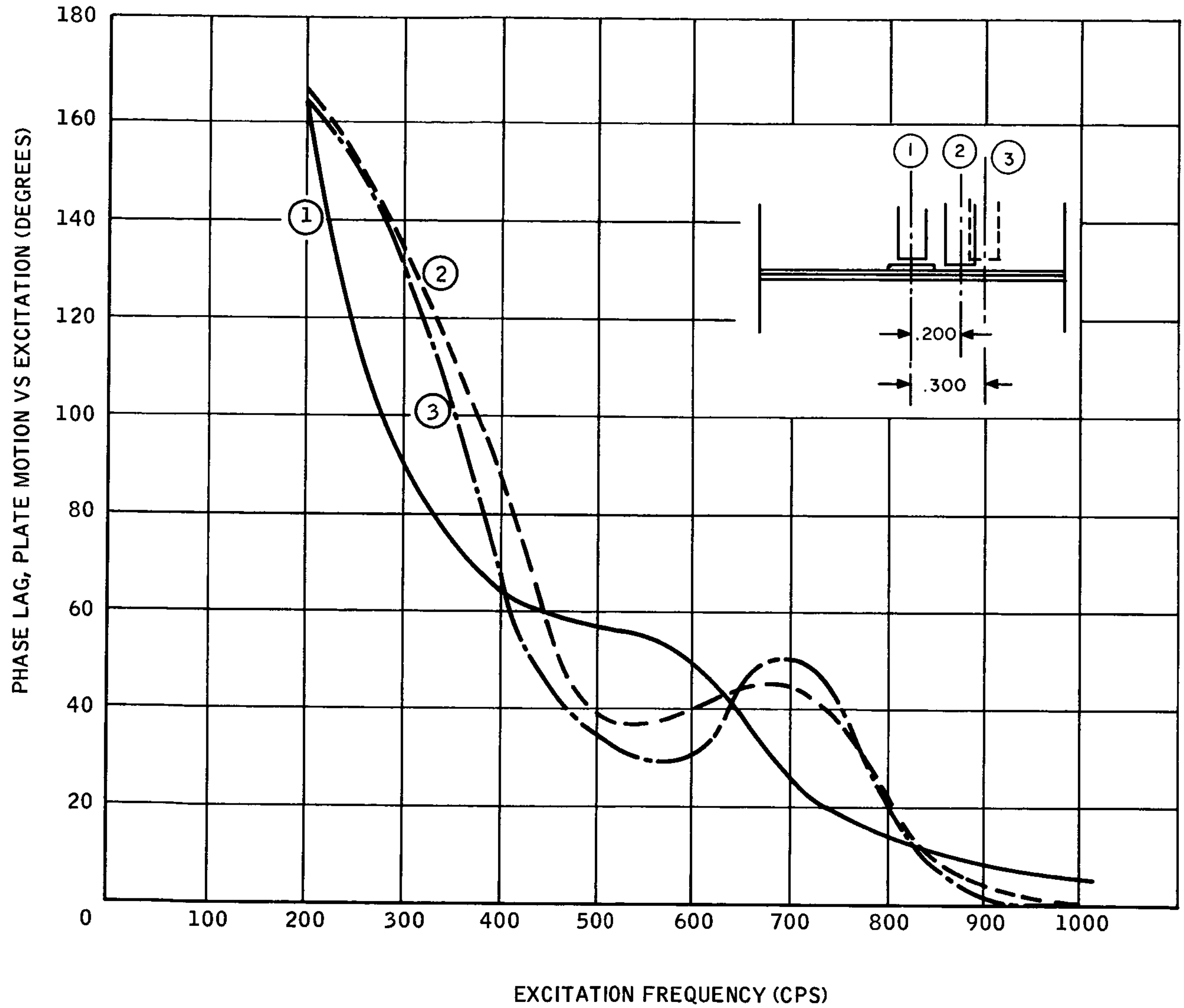

Figure 21. Plate Motion Phase Lag

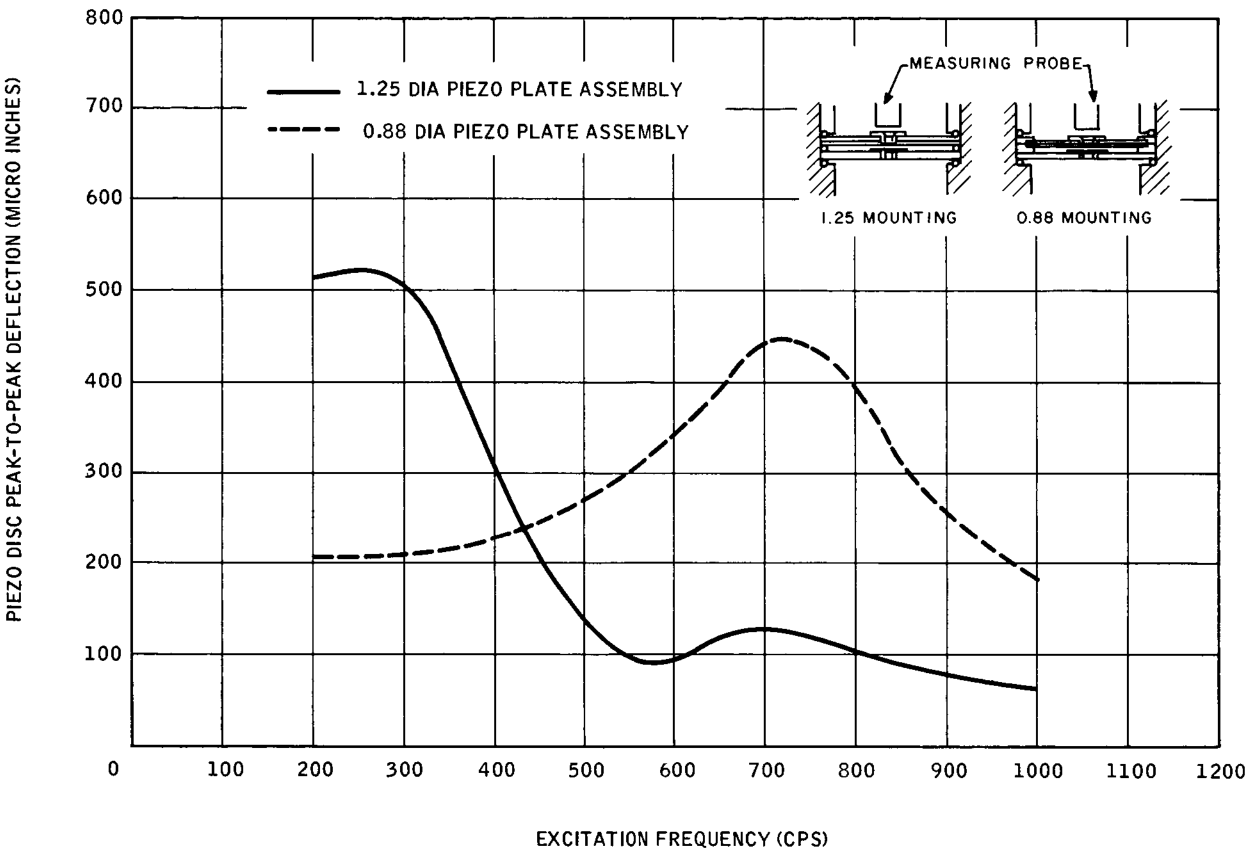

Figure 22. Piezo Plate Size versus Deflection

assembly. In a gyro assembly, maintenance of resiliency and stability of the 0-rings could be a problem under exposure to 300°F sterilization cycles. A special rubber (VITON or Flourosilicone type) will withstand exposure to 300°F for long periods of time in Kel F fluid.

Tests show that the silicone rubber (Honeywell Material Spec 7035) will withstand the 300°F sterilization requirement. Samples of this material were tested for 1000 hours at 300°F with a compression set of ~50 percent, a change in hardness of 28 percent, and small (~50 percent) dimensional changes.

Lead coating aluminum sealing rings can be used as an alternate plate mounting. These rings have the advantage of temperature stability and should not change pumping characteristics as mounting compliances can be matched to present pumping compliance.

PUMPING CHARACTERISTIC

Figure 23 shows the pressure flow relation for the 400-cps pump using the 1.25-inch diameter piezo dither disc assembly. This curve repeated quite well from assembly to assembly. Some degradation was noted if the assembly was loose but after nominal clamping of the assembly further clamping pressure had very little effect on pump performance.

Figure 24 shows the test mockup used to obtain the pump characteristics. The restrictor needle valve was used to set various output pressures for which simultaneous flows were read.

PIEZOELECTRIC PUMP POWER CONSUMPTION

Table 3 shows the power and current required to drive the 400-cps pumping plate at 50, 75, and 100 volts. The power measurements were made with the plate operating in the test mockup.

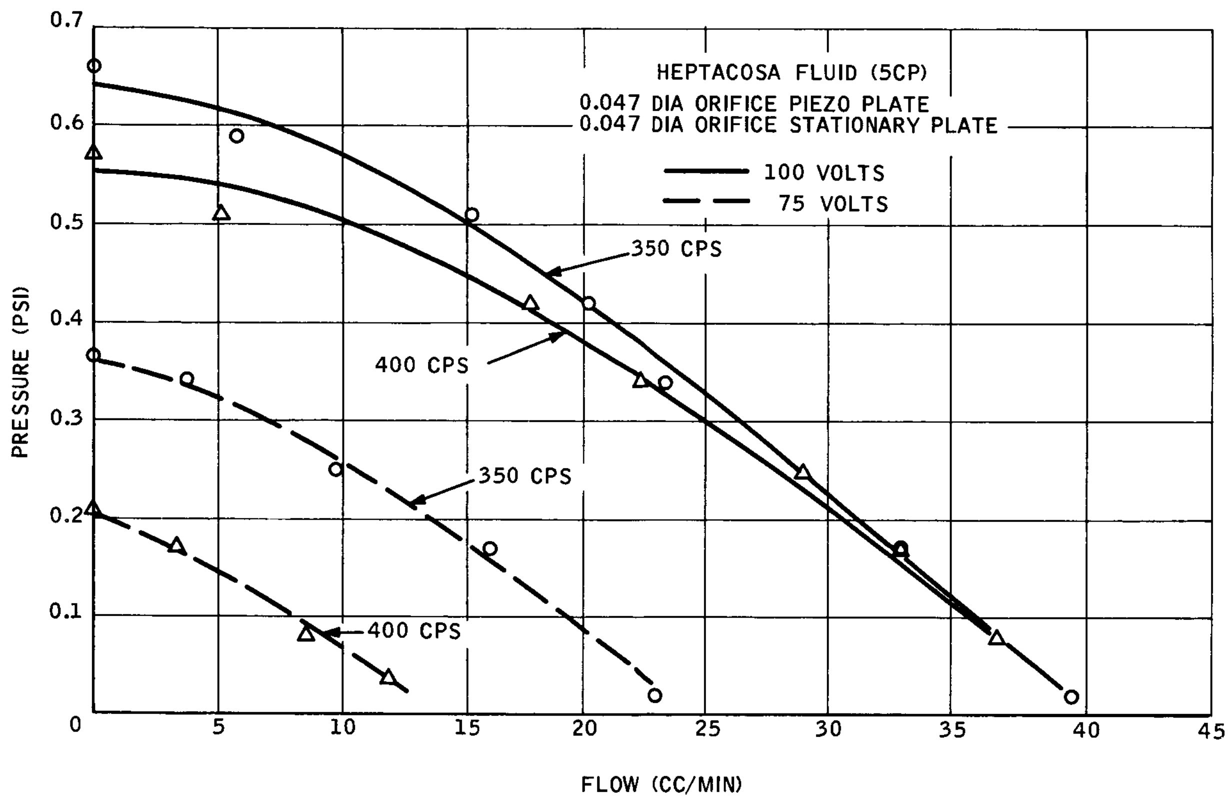

Figure 23. Piezoelectric Pump Characteristics

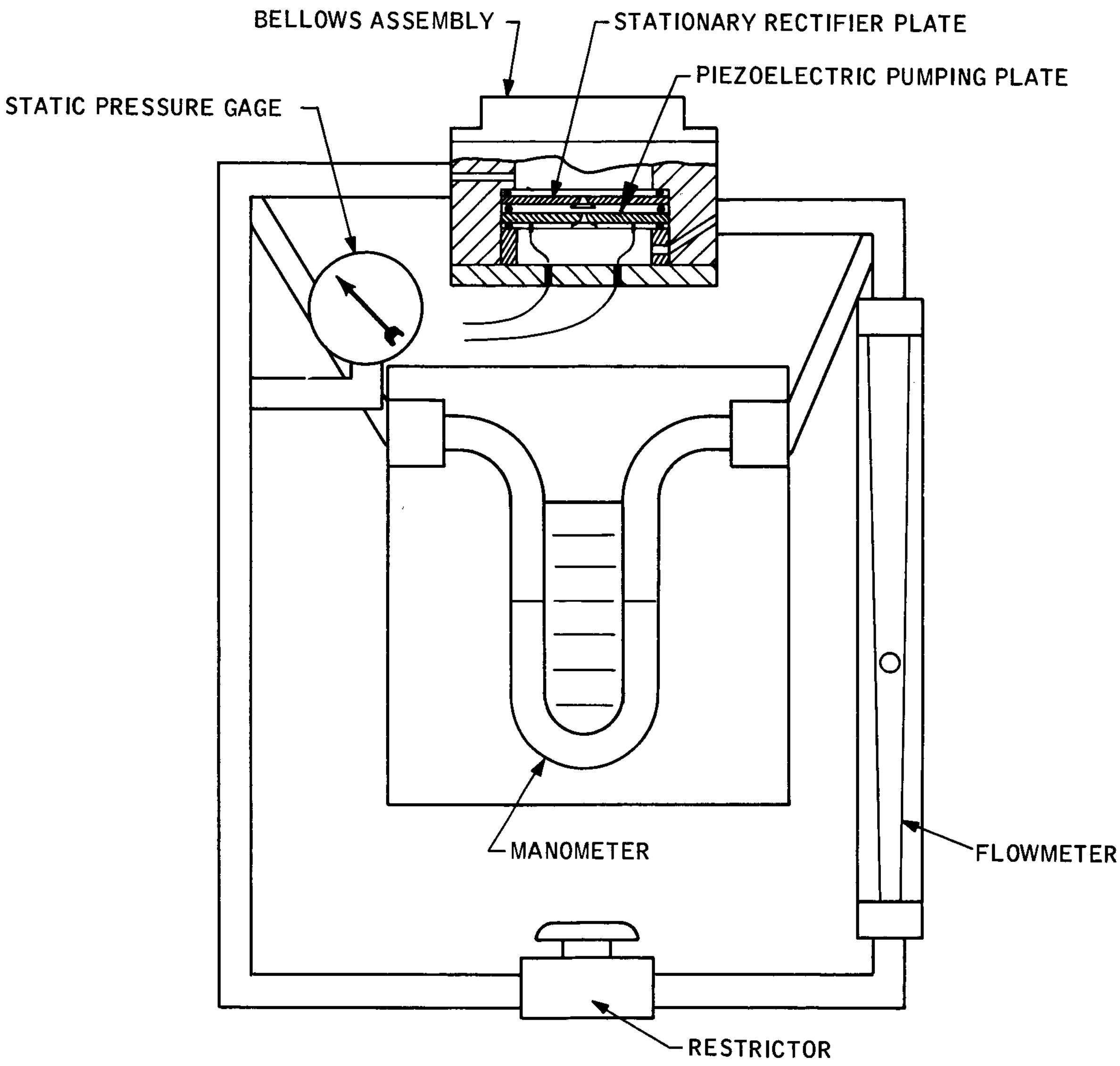

Figure 24. Piezoelectric Pump Test Mockup

Table 3. Power and Current Requirements

Frequency	Volts	Milliamperes	Watts
200	100	4.5	0.08
	75	3.1	0.032
	50	1.8	0.013
400	100	7.4	0.18
	75	5.0	0.08
	50	3.0	0.022
800	100	15.3	0.20
	75	10.6	0.09
	50	6.5	0.023

SECTION VI
NOMENCLATURE

A	Ratio, groove clearance to land clearance of rotary pump
D_R	Rotor drag dyne-cm
D	Gimbal damping, dyne-cm-sec
F_A	Gimbal axial support, lb. or grams
F_R	Gimbal radial support, lb. or grams
h_1	Radial step clearance, in.
h_2	Radial land clearance, inc.
h_3	End land clearance, in.
h_g	Groove clearance of rotary pump, in.
h_1	Land clearance of rotary pump, in.
K	Ratio, step length to step plus land length
L	Length of step length plus land length
N	Speed, rpm
P	Pressure, psi
P_o	Output pressure of pump, psi
Q	Fluid flow, in^3/sec or cc/min
Q_t	Total fluid flow
r_g	Gimbal radius to clearances, in.
r_1	Output radius of gimbal end land, in.
r_2	Inside radius of gimbal end land, in.
r_o	Outside radius of gimbal end surface, in.
R	Radius of rotary pump element, in.

T	Torque, gm-cm
α	Ratio, gimbal step clearance to gimbal land clearance
β	Rotary pump helix angle, deg
γ	Ratio, groove length to groove plus land length of rotary pump
ϵ	Eccentricity ratio of gimbal
ω	Angular velocity, radians/sec
μ	Viscosity, $lb\text{-}sec/in^2$ or centipoises
μ_p	Permeability
ρ	Density, grams/cubic centimeters

SECTION VII
REFERENCES

1. Honeywell Memo, "Hydrostatic Gimbal Suspension (Torsional Stiffness)", R. G. Baldwin from R. F. Anderson, dtd. 6 August 1963.

2. Honeywell Memo, "Hydrostatic Gimbal Bearing Analysis", R. G. Baldwin from R. Plunkett, dtd. 7 August 1963.

3. Honeywell Memo, "Axial Stiffness and Fluid Torques in Hydrostatic Stepped Bearings", R. G. Baldwin from R. Plunkett, dtd. 22 August 1963.

4. MTI Report 63TR52, "On the Spiral-Grooved, Self-Acting, Gas Bearing" by J.H. Vohr and C.H.T. Pan, dtd. January 1964.